A SIMPLIFIED METHOD OF SYNTHESIZING LADDER NETWORKS WITH IMAGE-PARAMETER HALF-SECTIONS

By

DAVID SILBER

A DISSERTATION PRESENTED TO THE GRADUATE COUNCIL OF
THE UNIVERSITY OF FLORIDA
IN PARTIAL FULFILLMENT OF THE REQUIREMENTS FOR THE
DEGREE OF DOCTOR OF PHILOSOPHY

UNIVERSITY OF FLORIDA

August, 1960

ACKNOWLEDGMENTS

The author would like to express his gratitude to the members of his supervisory committee for their advice and helpful criticism. He is especially indebted to Dr. T. S. George for his supervision and constant guidance, to Dr. W. H. Chen for his many valuable suggestions and to Dr. H. A. Meyer, Director of the Statistical Laboratory, for his help in obtaining numerical data by using the University's electronic computer.

TABLE OF CONTENTS

LIST OF TABLES

LIST OF ILLUSTRATIONS

CHAPTER I

INTRODUCTION

1.1 The Use of Frequency Selective Networks and Terminology

While transmitting information in the form of electrical signals from one point to another, we are faced with the problem of recovering a desired signal from undesired ones and from electrical noise.

When the energies of different signals are in different frequency regions, or bands (a situation which is often found in nature, or can be attained by various techniques in the process of converting the information into an electrical signal at the transmitting points), the separation of one signal from others makes use of the differences in energy-frequency spectra of different signals.

This separation is accomplished by placing some device in the path of the signal (before it reaches the receiving point) which exhibits frequency selective characteristics, i.e., a device which is capable of accentuating (or letting pass through without change) one frequency band, the band containing all or most of the energy of the desired signal, while suppressing (or attenuating) another band.

The device usually employed for this purpose consists of an array of electrical components (resistance, capacitance and

inductance) interconnected in a fashion which produces the desired frequency selectivity. There are some mechanical devices with this characteristic which are sometimes used.

A word on terminology: An array of interconnected electrical components is called an "electrical network," or in short a "network." The manner of interconnection of components, the choice of their type and number required in order to produce a specified electrical characteristic (e.g., frequency selectivity), as well as the mathematical tools employed in network problems, are treated in network theory.

If a network consists of electrical components, the values of which are independent of frequency, it is a "linear network"; if the circuit element values are positive constants, it is a "linear passive network."

A network inserted in a communication path, which usually consists of two wires, must have two input terminals and two output terminals, hence falls in the category of "four-terminal networks," or, more precisely, "two terminal-pair networks." A four-terminal network which has frequency discriminating properties is called an "electric wave filter," or in short, a "filter." Depending on the region of frequencies a filter favors or attenuates, there are "low-pass filters" (i.e., these filters pass low frequencies while attenuating high frequencies), "high-pass filters," "band-pass filters," "band-elimination filters" and "multiple pass-band filters" where a filter has several passbands separated by attenuation bands.

The external characteristics of a linear passive four-terminal network may be completely described by a set of three independent parameters, which are in general functions of frequency. Of the possible sets of parameters, there are some which can be readily obtained by measurement at the terminals without knowledge of the internal structure of the network; these are the open-and short-circuit impedances. A very convenient set of parameters, the "image parameters," may be obtained as functions of the open- and short-circuit impedances. The image parameters consist of two image impedances and an image transfer coefficient.

The external electrical characteristics of a filter inserted in a communication path between transmitting point (generator) and receiving point (load) are the operating characteristics called "insertion characteristics"; these consist of "insertion loss" and "insertion phase-shift" characteristics. The first is a measure of the decrease in amplitude of a sinusoidal voltage passing through the filter, the second gives the amount of phase shift (or delay) for a sinusoidal voltage passing from input to output (i.e., from generator to load) terminals of the filter. Both are, in general, functions of frequency.

1.2 The Image Parameter Method of Network Synthesis

The problem of designing a filter is to synthesize a network having a prescribed insertion loss characteristic.

There are two distinctly different methods of filter

design available. The older one, developed by Zobel[1*] from earlier work of Pupin, Campbell and Foster[2], is based on image parameter theory; the resulting image parameter filter is called a Zobel filter. The newer method, originated by Darlington,[3] is based on insertion loss theory developed independently by Darlington, Cauer and Piloty[4] at the same time.

The outstanding feature of the image-parameter design method is its simplicity. This, coupled with the fairly well performing filters obtainable by the image parameter design techniques, caused this method to be used almost exclusively in practical filter design.

The simplicity of this method stems from the "building block" structure of composite filters. Each "building block," or "section," is a four-terminal network which can be fully described by two image impedances Z_{I1} and Z_{I2} and an image transfer coefficient $\theta_I = \alpha_I + j\beta_I$, where α_I is the image attenuation coefficient and β_I is the image phase shift coefficient.

A composite filter is formed by connecting sections in tandem, with image impedances that are equal to each other (matched) at the terminals of the sections which are joined. The total transfer coefficient of the composite filter is simply the sum of the transfer coefficients of individual sections.

If these filters could be terminated at both ends by the respective image impedances (i.e., matched at the ends), the image

---

*Raised numbers refer to entries in the References at the end of this dissertation.

transfer coefficient would describe their actual (measurable) performance. However, since the image impedances are generally functions of frequency, and since the terminating impedances are usually constant resistances, the filters cannot, in general, be matched at the termination. This mismatch causes the quantities of interest, the insertion loss and insertion phase, to be somewhat different from the image attenuation and image phase shift.

Moreover, the requirement of matched image impedances at the points of interconnection of individual sections imposes restrictions on the networks obtainable by the image parameter method, as well as on their performance characteristics (i.e., their insertion loss and insertion phase characteristic). These restrictions lead to an inefficient use of network components.

1.3 The Insertion Loss Method of Network Synthesis

The insertion loss method of filter design is characterized by the fact that filters obtainable by it have an insertion loss characteristic exactly as prescribed, when inserted between prescribed terminations (hence the name "insertion loss theory"). It is based on the treatment of the entire problem of finding a four-terminal network satisfying given insertion loss requirements. The insertion parameters, rather than the image parameters of Zobel filters, are the primary design parameters from which the circuit element values of the filter are obtained in the last step of a sequence of (often lengthy) operations. The resulting filter, no matter how complicated, is obtained as an entity, rather than an aggregate of

individual building blocks (sections) as in Zobel filters, hence it does not suffer from the matching restrictions imposed on Zobel sections and permits the realization of optimum (in the sense of the number of circuit elements required to meet prescribed characteristics, and the element values) networks.

Another very desirable feature of the insertion loss method is the correction for incidental dissipation it permits. Though the range of compensation is limited by the type of insertion loss function (more specifically, by the distance of the nearest insertion-loss zero to the $j\omega$-axis in complex plane), it permits taking into account losses in components for a great number of cases encountered in practice.

1.4 Comparison of the Image Parameter and Insertion Loss Methods

A comparison of the image parameter method and the insertion loss method of network synthesis reveals that the latter is much more flexible in the results it produces, and much more sophisticated in the overall approach and in the mathematical tools it employs. As a result of the last, it is taught in most engineering schools only in graduate curricula, and the majority of practical design engineers have no opportunity to acquire a working knowledge of the insertion loss method while in school.

An important economical disadvantage of the insertion loss method of network synthesis, as compared with the image parameter method, is the much longer design time required by the insertion

loss techniques, resulting in a more costly filter design than in the case of image parameter filters.* On the other hand if the filter designed by the insertion loss method is more economical** than a corresponding Zobel filter (which is often the case), the increased cost of design may be offset when it is to be manufactured in large volume.

The situation in the practical filter-design field may be summarized as follows: Because of the simplicity of the design procedures and of the acceptable filters the image parameter method yields, and because of the more analytical background and longer design time required of the designers using the insertion loss method, the image parameter method is still used by the majority of design engineers, though using the insertion loss method may often result in a better filter.

There have been many contributions in the past to both design methods;*** a great number of these aimed at bridging the gap existing between modern theory and practical design methods. The approach from the image-parameter field is, in general, toward the improvement of Zobel filters by better matching, e.g., Ref. 6, by reduction of components in derived terminations, e.g., Ref. 7, or by finding new structures, e.g., Ref. 8. In the insertion loss field the emphasis

---

*The design time may be reduced by employing modern means of computation, e.g., an electronic computer. This, while reducing the required design time, will not, in general, reduce the overall design cost.

**An economical filter is one that requires fewer or less expensive components, or its component values may have higher tolerances without upsetting the performance, etc.

***For a summary of recent contributions and a good list of references, see Ref. 5.

is on a more comprehensive presentation of known material,[9] on simplification of design techniques,[10] and on tabulation of designs.[11, 12]

This dissertation is concerned with a synthesis method for ladder networks which employs "building blocks" similar to the image parameter filter; in fact, the "elementary building block" used is an image parameter half-section. To form a composite filter these "building blocks" are connected in tandem in a fashion similar to a Zobel filter, without, however, the fundamental restriction of Zobel filters, that of matching image impedances at the points of interconnection.

1.5. Statement of Objectives

The objectives of this dissertation are two-fold:

1. The introduction and investigation of a new method of synthesis of ladder networks by which filters can be designed with a simplicity similar to the simplicity of the image parameter method of design, yet yielding more general filters than the Zobel filter of the image parameter method (i.e., yielding filters the choice of element values and the performance characteristics of which do not have the limitations of Zobel filters).

2. The derivation of relations and determination of parameter values for use in this synthesis method, by which

design engineers familiar only with the image parameter method will be able to design filters with desirable insertion loss characteristics (Butterworth, Tchebycheff and elliptic-function type) until now obtainable primarily by the insertion loss method.

The contents of this dissertation is divided into three chapters. Chapter II deals with methods of interconnection of the elementary building blocks. It is shown that any lossless ladder can be expressed in terms of image impedance half-sections with one common image parameter. The cut-off frequency is chosen as the common parameter.

In Chapter III some methods of finding the image parameters of the elementary building blocks are investigated. The image parameters are then determined for two-section ladder filters having Butterworth, Tchebycheff, and elliptic-function insertion loss characteristics.

Based on results of Chapter III, a modification of Zobel filters is introduced in Chapter IV. This modification permits control of the distortion in passband of Zobel filters; it also makes the economy of these filters (as far as the performance per number of elements is concerned) comparable to the economy of optimum filters.

CHAPTER II

THE GENERAL LADDER NETWORK IN TERMS OF ELEMENTARY BUILDING BLOCKS CONNECTED IN TANDEM

2.1. The Elementary Building Block

Only the low-pass ladder will be considered here, since the high-pass, band-pass and band-elimination networks can be obtained from the low-pass ladder by well known frequency transformations.[13, 14]

The elementary building block (Fig. 2.1) is an image parameter m-derived low-pass half-section, the circuit element values of which are determined by the image parameters m, r and ω_c, using the simple relations from image parameter theory:[15]

$$c_1 = \frac{m}{r\,\omega_c} \tag{2.1}$$

$$h_2 = \frac{mr}{\omega_c} \tag{2.2}$$

$$c_2 = \frac{1 - m^2}{mr\,\omega_c} \tag{2.3}$$

$$m = \left[1 - \left(\frac{\omega_c}{\omega_\infty}\right)^2\right]^{\frac{1}{2}} \qquad 0 \leq m \leq 1 \tag{2.4}$$

where ω_c is the cut-off frequency of the half-section, r is the image impedance at zero frequency, ω_∞ is the frequency of infinite attenuation.

We also have (Fig. 2.2 and Fig. 2.3)

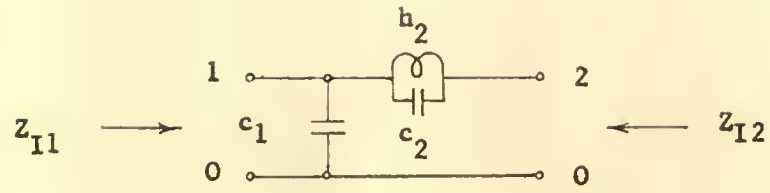

Fig. 2.1. The elementary building block

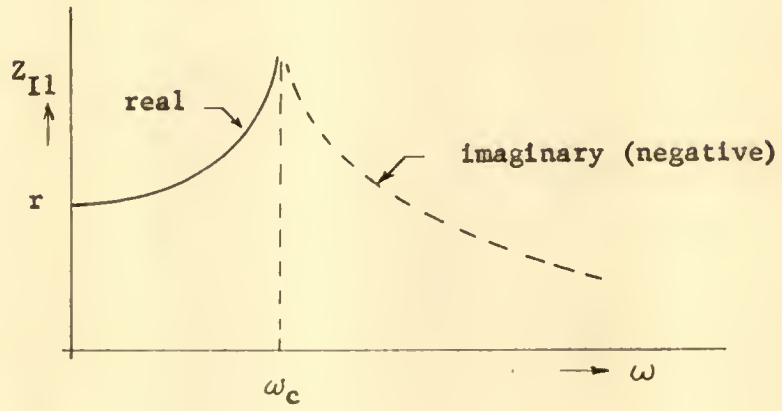

Fig. 2.2. Image impedance of the elementary building block at terminals 1--0 of Fig. 2.1.

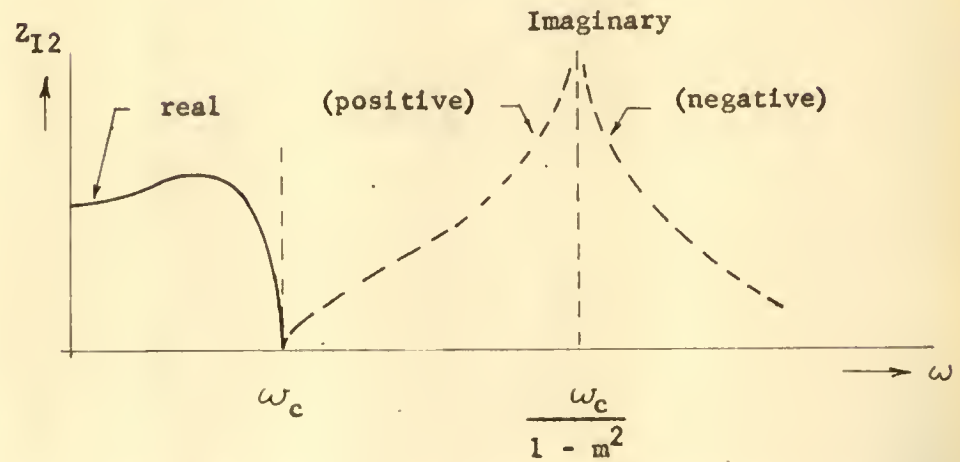

Fig. 2.3. Image impedance of the elementary building block at terminals 2--0 of Fig. 2.1.

$$Z_{I1} = \frac{r}{\left[1 - \left(\frac{\omega}{\omega_c}\right)^2\right]^{\frac{1}{2}}} \tag{2.5}$$

$$Z_{I2} = \frac{r\left[1 - \left(\frac{\omega}{\omega_c}\right)^2\right]^{\frac{1}{2}}}{1 - (1 - m^2)\left(\frac{\omega}{\omega_c}\right)^2} \tag{2.6}$$

Analysis of equations (2.1), (2.2), (2.3) and (2.4) reveals that the parameters m, r and ω_c uniquely determine the component values c_1, c_2 and h (with the restriction that m is a real and positive constant, $0 \leq m \leq 1$). On the other hand, given c_1, c_2 and h, the design parameters m, r and ω_c may be found from the following relations:

$$r^2 = \frac{h_2}{c_1} \tag{2.7}$$

$$m^2 = \frac{c_1}{c_1 + c_2} \tag{2.8}$$

$$\omega^2 = \frac{1}{h_2(c_1 + c_2)} \tag{2.9}$$

Equations (2.7), (2.8) and (2.9) are obtained from equations (2.1), (2.2) and (2.3) solved for r, m and ω_c. Restricting the design parameters to be positive, it is seen from the last set of equations that c_1, c_2 and h_2 uniquely determine the design parameters r, m and ω_c.

2.2. Methods of Connecting the Elementary Building Blocks

Fig. 2.4 shows one method of connecting the half-sections

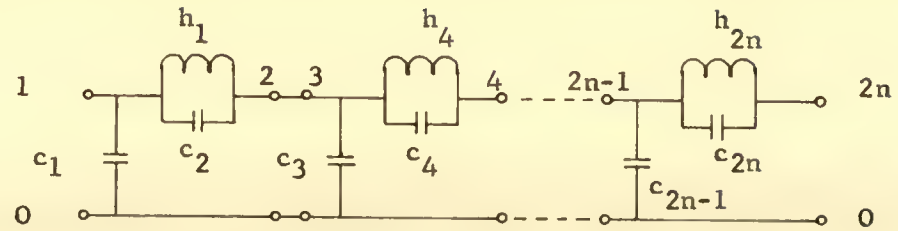

n = number of half-sections

Fig. 2.4. Tandem connection of the elementary building blocks giving a non-symmetrical ladder filter

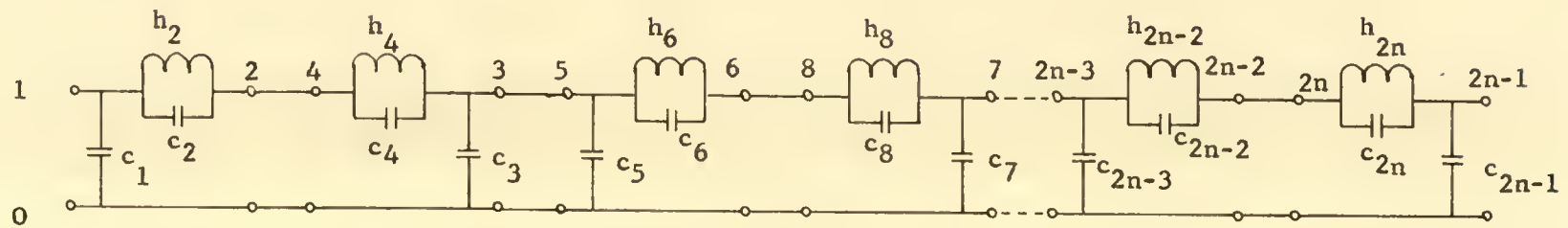

n = number of half-sections

Fig. 2.5. Connection of the elementary building blocks by which symmetrical and non-symmetrical ladder filters may be obtained

into a ladder network; here we connect the even-numbered terminals with the odd-numbered ones. We note that the even-numbered terminals have an image impedance given by equation (2.5) (i.e., the image impedance between the even-numbered terminals and 0, the common, for one half-section only, is given by (2.5)), and the odd numbered terminals have an image impedance given by equation (2.6), hence we connect the terminal pairs having different types of image impedances.

The image impedance at both terminations of the resulting ladder will not be of the same type; the image impedance at terminals 1-0 is of the type given by equation (2.5), the constant-k mid-shunt type, whereas, the image impedance at the other termination (at terminal pair 2n-0) is of the type given by equation (2.6), the m-derived mid-series type. Therefore the resulting ladder cannot be symmetrical.*

Another method of connection is shown in Fig. 2.5, where we connect even-numbered terminals with even-numbered terminals and odd-numbered terminals with odd-numbered ones, i.e., we connect pairs of terminals having image impedances of the same type.

If the ladder contains an even number of half-sections, both image impedances at the terminations will be of the same type, hence the ladder can be symmetrical. If the number of half-sections is odd, the image impedances at the terminations are similar to those of Fig. 2.4. The method of connection shown in Fig. 2.5 results then in

---

*A 4-terminal network possesses electrical symmetry if the image impedances at both terminal-pairs are equal, i.e., one terminal pair cannot be distinguished from the other pair by external measurements.

a more general ladder than the connection of Fig. 2.4 (in fact, Fig. 2.4 can be considered as a special case of Fig. 2.5 in which the components of the second, fourth, etc., section are zero, i.e., $h_4 = h_8 = h_{12} = \cdots = h_{2n} = 0$ and $c_3 = c_7 = \cdots = c_{2n-1} = 0$) hence this method of connection will be used in subsequent analysis. Since every component of this ladder can assume any value depending on the choice of the image parameters r_1, m_1, ω_{c1}, r_2, m_2, ω_{c2}, ... r_n, m_n, ω_{cn}, it is clear that the reverse must hold also, i.e., any ladder network having the configuration of Fig. 2.5 can be synthesized with image parameter half-sections by proper choice of the image parameters r_i, m_i and ω_{ci}.

2.3. A Conventional Low Pass Ladder in Terms of Elementary Building Blocks

A particular case of the ladder of Fig. 2.5, one in which a reduction in the number of components can be realized, would result if two adjacent parallel resonant circuits in the series branches of the ladder could be combined into one parallel resonant circuit. Obviously this can be accomplished only if the resonant frequencies of the adjacent circuits are equal. The resulting ladders are shown in Fig. 2.6 (a) and (b), where the components of Fig. 2.5 combine as follows:

$$q_1 = c_1 \tag{2.10}$$

$$q_2 = h_2 + h_4 \tag{2.11}$$

$$a_2 = \frac{c_2 c_4}{c_2 + c_4} \tag{2.12}$$

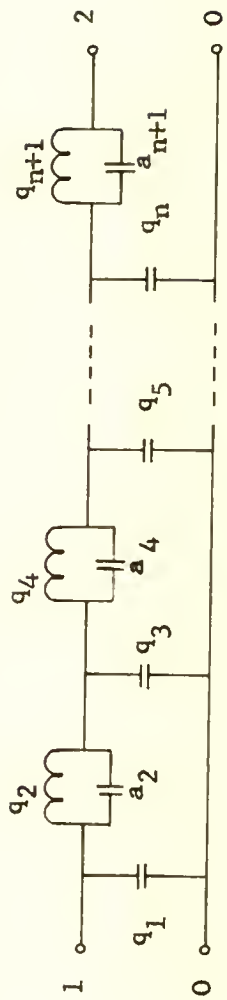

n = an odd number

(a)

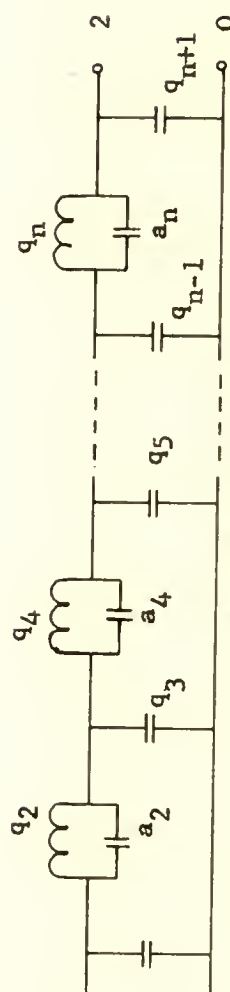

n = an even number

(b)

Fig. 2.6. A special case of the ladder of Fig. 2.5

$$a_2 q_2 = \frac{1}{\omega_{2\infty}^2} = h_2 c_2 = h_4 c_4 \tag{2.13}$$

$$q_3 = c_3 + c_5 \tag{2.14}$$

$$q_4 = h_6 + h_8 \tag{2.15}$$

$$a_4 = \frac{c_6 c_8}{c_6 + c_8} \tag{2.16}$$

$$a_4 q_4 = \frac{1}{\omega_{4\infty}^2} = h_6 c_6 = h_8 c_8 \tag{2.17}$$

In Fig. 2.6 (a) the ladder consists of an odd number of half-sections (the number of half-sections = n = odd), hence (see Fig. 2.5)

$$q_{n+1} = h_{2n-2} \tag{2.18}$$

$$a_{n+1} = c_{2n-2} \tag{2.19}$$

The ladder of Fig. 2.6 (b) has an even number of half sections (n=even), hence here (see Fig. 2.5)

$$q_n = h_{2n} + h_{2n-2} \tag{2.20}$$

$$a_n = \frac{c_{2n-2}\, c_{2n}}{c_{2n-2} + c_{2n}} \tag{2.21}$$

$$a_n q_n = \frac{1}{\omega_{n\infty}^2} = h_{2n} c_{2n} = h_{2n-2} c_{2n-2} \tag{2.22}$$

$$q_{n+1} = c_{2n-1} \tag{2.23}$$

The number of image parameters for the ladders of Fig. 2.6

is 3n (three parameters, r_i, m_i and ω_{ci}, for each of the n half-sections). However, due to the conditions of equations (2.13), (2.17) ··· (2.22), some of the parameters will be related by these equations, resulting in the number of independent image parameters being equal to the number of components in the ladder.

Consider the problem of expressing a given ladder of the form of Fig. 2.6 in terms of image parameter half-sections, i.e., given a ladder of Fig. 2.6, determine the element values of an equivalent ladder of Fig. 2.5. One question arises immediately: Is there a unique equivalent of the ladder of Fig. 2.6 in the form of one of Fig. 2.5? If not, could there be one specific form of Fig. 2.5 which is advantageous?

The first question can be answered by noting that there are 3n components in ladder of Fig. 2.5, the values of which are to be determined from 2n + 1 relations.* Thus there is no unique equivalent of a ladder of Fig. 2.6 in the form of one in Fig. 2.5

The second question can be answered after investigating the possible equivalent ladders of the form of Fig. 2.5.

---

*For a ladder of Fig. 2.6 (a) we have three equations of the form of equation (2.11), (2.12) and (2.13) for each series branch except the last, i.e., 3(n - 1)/2 equations; one equation for each shunt branch, i.e., (n + 1)/2 equations ((n - 1)/2 of the form of (2.14) and one equation (2.10)), and two relations (2.18) and (2.19) for the last series branch, giving a total of 3(n - 1)/2 + (n + 1)/2 + 2 = 2n + 1. For Fig. 2.6 (b) we have 3n/2 equations of the form of (2.11), (2.12) and (2.13) for the series of the form of (2.11), (2.12) and (2.13) for the series branches, and (n + 2)/2 for the shunt branches, giving a total of 3n/2 + (n + 2)/2 = 2n + 1.

In order to obtain a particular ladder equivalent, $3n - (2n + 1) = n - 1$ component values of the equivalent ladder of Fig. 2.5 will have to be either chosen or specified by additional n-1 equations* (i.e., we have n-1 degrees of freedom). It is clear that the n-1 components, the values of which are arbitrary, will be located in the ladder in accordance with the location of the components in Fig. 2.6 which on division produce the n-1 degrees of freedom (e.g., one cannot choose arbitrarily the values of the first n-1 components, starting with c_1, c_2, h_2, c_4, h_4 ... up to the (n-1) - th component in Fig. 2.5).

Examination of the ladders in Fig. 2.6 shows that every branch of the ladder which is divided produces one degree of freedom, as shown by the symbol "1" in Fig. 2.7 (a). The arrows indicate where the degrees of freedom originate, hence they also indicate which of the elements may have arbitrary values.

Fig. 2.7 (b) and (c) show two possible choices of the location of arbitrary elements: In Fig. 2.7 (b) the first half-section has no arbitrary elements, the second has one in the series branch and one in the shunt branch, the third half-section has none, etc. In

---

*The chosen values of the components, though arbitrary in a certain range, should not result in a negative element lest some of the image parameters from which the half-sections can be computed become imaginary. If instead of a component value a corresponding image parameter is chosen, a similar limitation applies in addition to the requirement $0 < m \leq 1$ (or $\omega_c < \omega_\infty$).

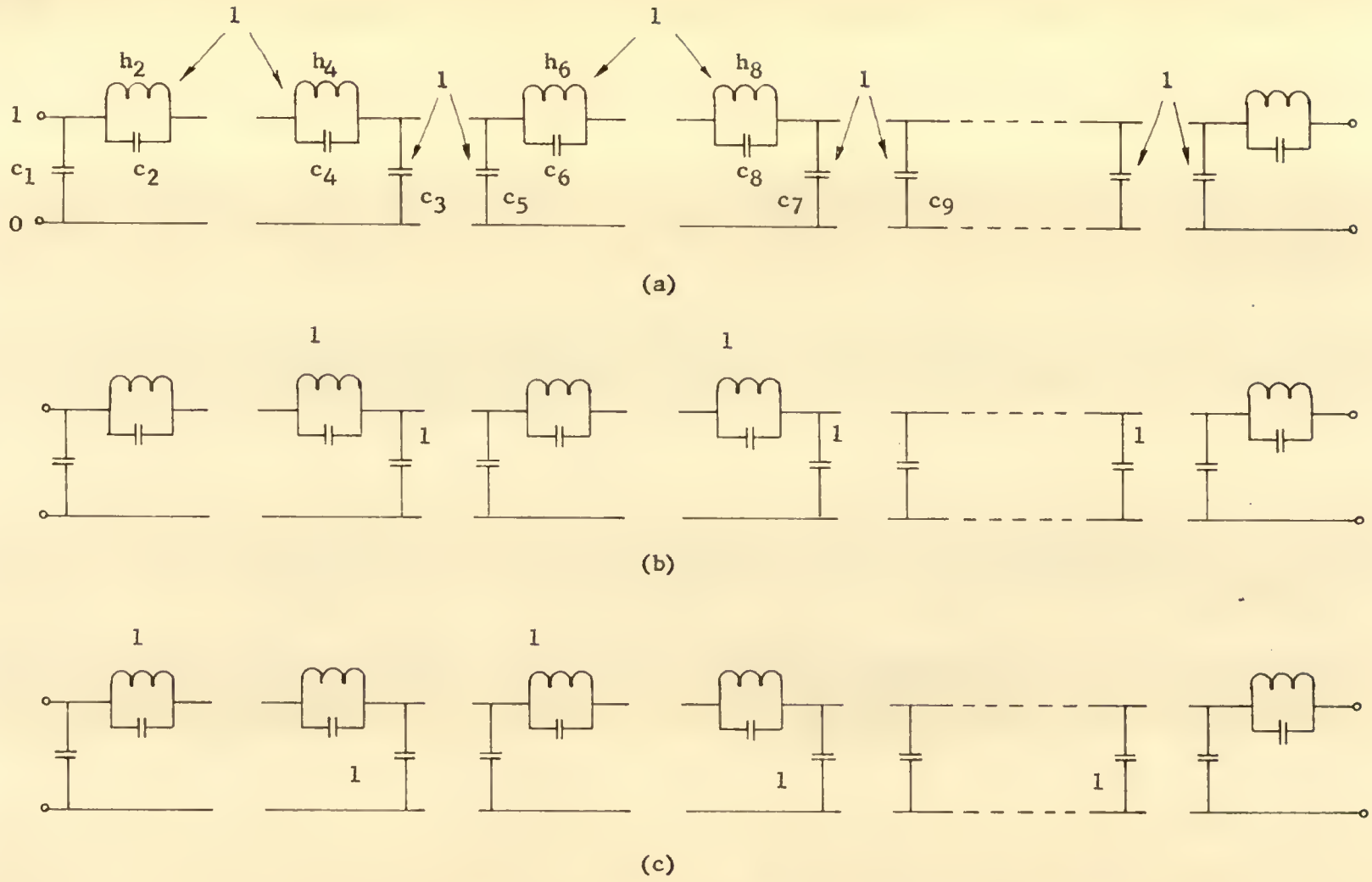

Fig. 2.7. Possible locations of elements with arbitrary values

Fig. 2.7 (c) every half-section, except the last one, has one arbitrary element. There are a number of combinations of the arrangements in Fig. 2.7 (b) and (c) possible.*

The arrangement of arbitrary elements in Fig. 2.7 (c) appears advantageous in that it permits choice of the circuit element value of one component (or one parameter) in each half-section, except the last. Hence the resulting ladder, with the exception of one terminating half-section, can be made to have one arbitrary parameter.**

The values of the n-1 arbitrary elements may conveniently be specified by additional n-1 arbitrary equations, in which the limitations on the chosen values (see footnote* on previous page) could be included. A simple set of n-1 of such equations could be

$$p_1 = p_2 = p_3 = \cdots = p_n \tag{2.24}$$

where p denotes an image parameter.*** In particular if the same

---

*Similar reasoning applied to the ladder of Fig. 2.6 (b) shows that the conclusions reached in analysis of Fig. 2.6 (a) hold here as well; we may have one arbitrary element in each half section, except in one of the terminating half-sections.

**Since the component values of a half-section can be expressed in terms of image parameters r, m and ω_c, equation (2.1), (2.2) and (2.3), the fact that one of the component values can be chosen arbitrarily means that one of the image parameters can be chosen arbitrarily.

***We note that from equation (2.24) we have n-1 relations of the form $p_1 = p_2$, $p_1 = p_3$, $\cdots$ $p_1 = p_n$, hence the value of p cannot be chosen but is determined from 3n simultaneous equations, 2n + 1 of which are in the form of equation (2.10) to (2.23) with h's and c's substituted by equation (2.1) to (2.4).

image parameter is chosen for all p's, the resulting ladder will be very similar to an image parameter Zobel filter[1, 15, 16] when p denotes either r or ω_c.*

A convenient choice for p, equation (2.24), is to let it denote the cut-off frequency ω_c, i.e., letting the cut-off frequencies of all n half-sections be equal. This would make the image parameters m equal for the half-sections with common parallel resonant frequencies ω_∞ (see equation (2.4)).

The above leads to the following conclusion:

Any conventional ladder filter, Fig. 2.6, can be synthesized by tandem connected (method of Fig. 2.5) image parameter half-sections, pairs of which have equal m-values and all of which have equal cut-off frequencies ω_c.

This is equivalent to stating that:

Any conventional ladder filter can be obtained from an image impedance Zobel filter by changing the impedance levels $r_1, r_2, \cdots r_n$ of its half-sections.

In Chapter III some methods will be investigated, by which the required impedance levels r_i, the cut-off frequency ω_c and the m-values could be determined so as to obtain a ladder filter having a prescribed insertion loss.

---

*A conventional image parameter filter is called a Zobel filter. It is a filter consisting of connected-in-tandem image-parameter sections or half sections (prototype or m-derived) with common cut-off frequencies ω_c, and with image impedances (see equations (2.5) and (2.6)) which match each other at the points of interconnection. In terms of our elementary building blocks, a Zobel filter will have $\omega_{c1} = \omega_{c2} = \cdots = \omega_{cn}$ and $r_1 = r_2 = \cdots = r_n$.

2.4. Filters with Incidental Dissipation in Terms of Elementary Building Blocks

One of the major disadvantages of the image parameter Zobel filter design technique is the fact that dissipation cannot be taken in account in design (though the effect of dissipation may be found by analysis).

The modern network theory offers a technique[3] which allows one to synthesize a filter with dissipation producing the same form of insertion loss curve as one without dissipation, except for an additional constant (independent of frequency) loss. This technique, called predistortion, is based on the effect of dissipation on the location of poles and zeros of the insertion voltage ratio in the complex frequency plane.

Given the pole and zero distribution of a desired insertion voltage ratio of a dissipationless ladder filter, e.g., Fig. 2.8 (poles and zeros on solid curve), the addition of positive resistance to each component (in series with an inductance and in parallel with a capacitance) in such amounts that would make the Q-factors of all components equal, would move the zeros and poles in Fig. 2.8 horizontally a distance $d = 1/Q$ to the left, as indicated by the poles and zeros located on the dashed curve. Adding negative resistance to the dissipationless components in the same amounts as above would shift the poles and zeros a horizontal distance d to the right, as indicated by the zeros and poles on the dotted curve* (the dotted

*This horizontal shift is equivalent to transforming the complex variable $s = \sigma + j\omega$ to $s \pm d$, where the (+) and (-) signs correspond to addition of positive or negative resistance, respectively.

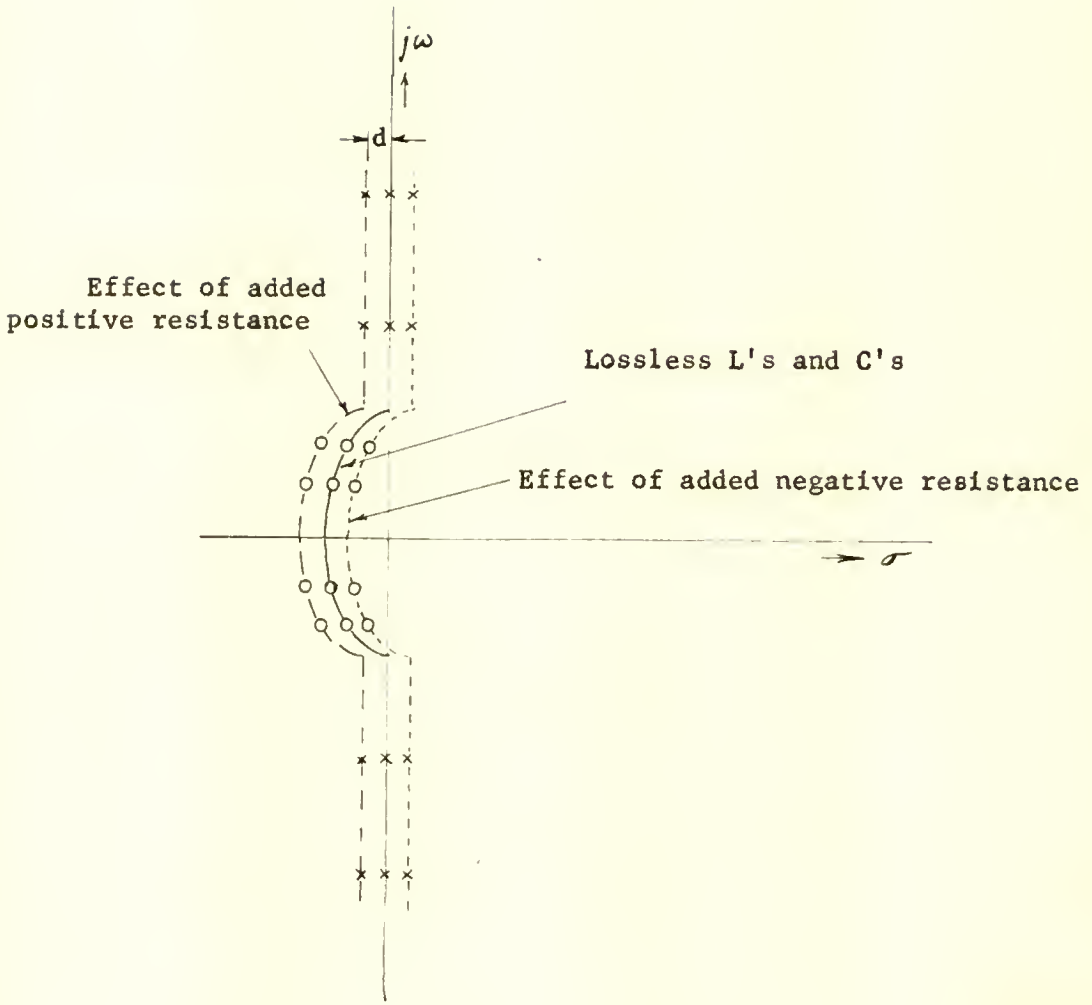

Fig. 2.8. Effect of adding proportionately equal amounts of resistance on the location of poles and zeros of the insertion voltage-ratio function

curve is called the predistorted curve for an amount of dissipation equal to d).

Suppose that the pole and zero distribution on the dotted curve is used to synthesize a dissipationless ladder network.* If now dissipation d is added to each element, the poles and zeros would move to the left a horizontal distance d and the distribution on the solid curve (Fig. 2.8) would be obtained, resulting in the desired insertion loss.

The lossless ladder obtained from the predistorted curve (dotted curve) can be represented by elementary building blocks (image parameter half-sections) as outlined in section 2.3. The image parameters r, m and ω_c of these building blocks will in general not be equal to the image parameters of the building blocks corresponding to a ladder synthesized from the pole and zero locations on the solid curve (the pole and zero location of the desired insertion voltage ratio).

Thus, given a lossless ladder filter in terms of image parameters r, m and ω_c, the effect of predistortion for a certain amount of dissipation can be obtained by a corresponding (to the amount of dissipation) change in the image parameters r, m and ω_c of the elementary building blocks.

---

*In practice, predistortion is applied to the zeros only, since the application to the poles would result in a network function which is not realizable by a lossless passive ladder without mutual (inductive) coupling. Thus the transformation of s to s-d is applied only to the numerator of the insertion voltage ratio function, and compensation of the effects of dissipation for the passband only is achieved. Note also that there is an upper limit of d, which must be smaller than the horizontal distance of the nearest zero to the $j\omega$-axis, for physical realizability with passive networks.

CHAPTER III

DERIVATION OF THE IMAGE PARAMETERS FOR LADDER FILTERS HAVING PRESCRIBED INSERTION LOSS CHARACTERISTICS

In this chapter the image parameters will be determined for the elementary building blocks which, when connected in tandem, result in ladder filters with Butterworth (maximally flat) Tchebycheff (equal ripple in passband only), and elliptic function (equal ripple in passband and in stopband) insertion loss characteristic. The image parameters will be expressed in terms of the critical frequencies (poles and zeros) of the insertion loss function. The investigation will be limited to two-section symmetrical filters.

3.1. Outline of Approach

The insertion loss L (in db) as a function of normalized frequency ω for the above three types of response is given by[17]

$$L = 10 \log (1 + E^2) \qquad (3.1)^*$$

where E denotes a polynomial or a ratio of two polynomials in ω, the form and the coefficients of which determine the type of response. The zeros and poles of $E(\omega)$ coincide with the zeros and poles of the insertion loss function $L(\omega)$, as can be seen from equation (3.1). It shall then be attempted to express the

---

*Equation (3.1) is for symmetrical filters only; it will be assumed for convenience that the filter is working between equal resistances of 1 ohm.

image parameters of the elementary building blocks in terms of these poles and zeros.

Method I:

One way of accomplishing this could be to find the insertion loss of a ladder consisting of elementary building blocks in terms of the image parameters of its half-sections. Comparison of this insertion loss with the insertion loss of Butterworth, Tchebycheff or elliptic-function type would yield a number of equations which, when solved simultaneously, would give the image parameters m, r and ω_c in terms of the poles and zeros of the insertion loss function.

Method II:

Another method of getting the same results for specific numerical cases would be to synthesize the ladder from the given insertion loss function by any suitable method (e.g., Darlington's method) and then express the ladder in terms of image parameter half-sections, obtaining a number of equations of the form of equations (2.10) to (2.23);* substituting for h's and c's equations (2.1) to (2.4), a set of equations in m_i, r_i and ω_c are obtained, which could be solved (at least theoretically) simultaneously for the image parameters.

The first approach is more general and will be used here.

---

*It is to be noted here that q_i and a_i are known.

Some numerical data will be obtained using the second approach.

3.2. Insertion Loss of a Two-Section Ladder Filter in Terms of Image Parameters

The two section symmetrical ladder which will be used in subsequent investigation is shown in Fig. 3.1.* This ladder is obtained by tandem connection of image parameter half-sections as shown in Fig. 3.2.

Comparison of the ladders of Fig. 3.1 and 3.2 yields the following relations:

$$q_1 = \frac{m_{12}}{r_1 \omega_c} \qquad 1(3.2)$$

$$q_2 = \frac{m_{12}(r_1 + r_2)}{\omega_c} \qquad (3.3)$$

$$a_2 = \frac{1 - m_{12}^2}{r_{12} \omega_c (r_1 + r_2)} \qquad (3.4)$$

$$q_3 = \frac{1}{\omega_c}\left(\frac{m_{12}}{r_2} + \frac{m_{34}}{r_3}\right) \qquad (3.5)$$

$$q_4 = \frac{m_{34}}{\omega_c}(r_3 + r_4) \qquad (3.6)$$

$$a_4 = \frac{1 - m_{34}^2}{m_{34} \omega_c (r_3 + r_4)} \qquad (3.7)$$

$$q_5 = \frac{m_{34}}{r_4 \omega_c} \qquad (3.8)$$

---

*The Butterworth and Tchebycheff filter can be considered as a special case of the ladder of Fig. 3.1 in which $a_2 = a_4 = 0$.

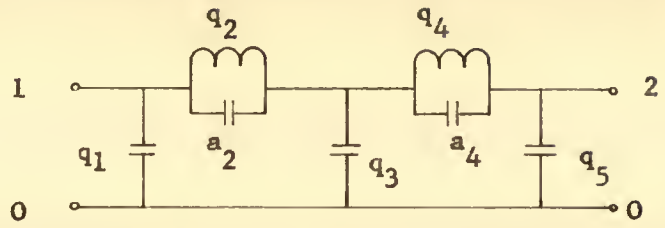

Fig. 3.1. A two section ladder filter

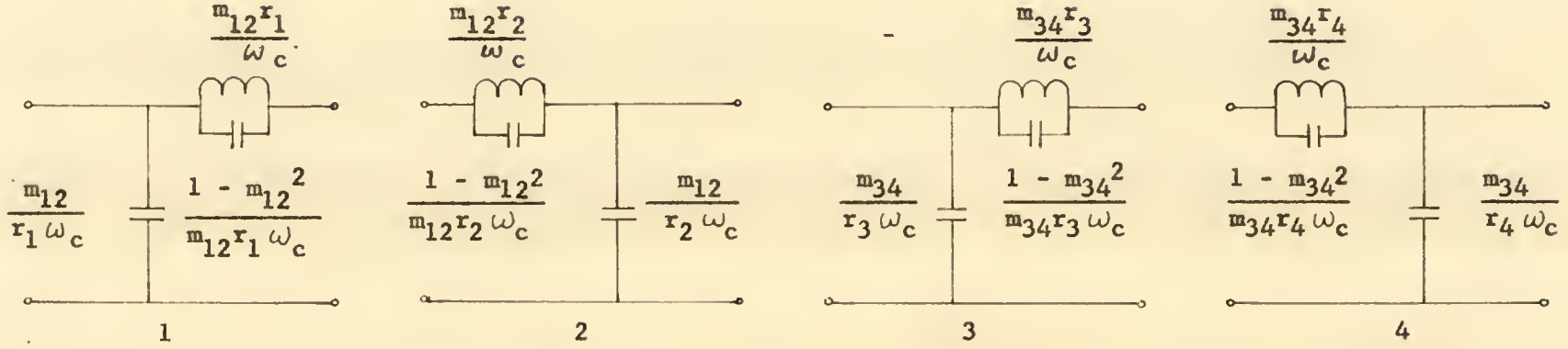

Fig. 3.2. Elementary building blocks from which the ladder of Fig. 3.1 may be obtained.

where r_1, r_2, r_3 and r_4 are the impedance levels of the half-sections 1, 2, 3 and 4, respectively; m_{12} is the common m-value of half-section 1 and 2; m_{34} is the common m-value of half-section 3 and 4; ω_c is the cut-off frequency common to all half-sections; q_1, q_3, q_5, a_2 and a_4 have dimensions of capacitance; and q_2 and q_4 have dimensions of inductance.

It is much more convenient to find the insertion loss of a lattice equivalent to the ladder of Fig. 3.1, rather than that of the ladder directly.

A lattice equivalent of the ladder of Fig. 3.1 is shown in Fig. 3.3 (a).

The series reactance X_a and the shunt reactance X_b of the lattice of Fig. 3.3 (a) are given by

$$X_a = \frac{Z_a}{j} = \frac{\omega}{A_1 - A_2\omega^2} \tag{3.9}$$

$$X_b = \frac{Z_b}{j} = \frac{1 - A_3\omega^2}{\omega(A_4\omega^2 - A_5)} \tag{3.10}$$

$$A_1 = \frac{1}{L_1} \tag{3.11}$$

$$A_2 = C_1 \tag{3.12}$$

$$A_3 = L_2C_2 \tag{3.13}$$

$$A_4 = L_2C_2C_3 \tag{3.14}$$

$$A_5 = C_2 + C_3 \tag{3.15}$$

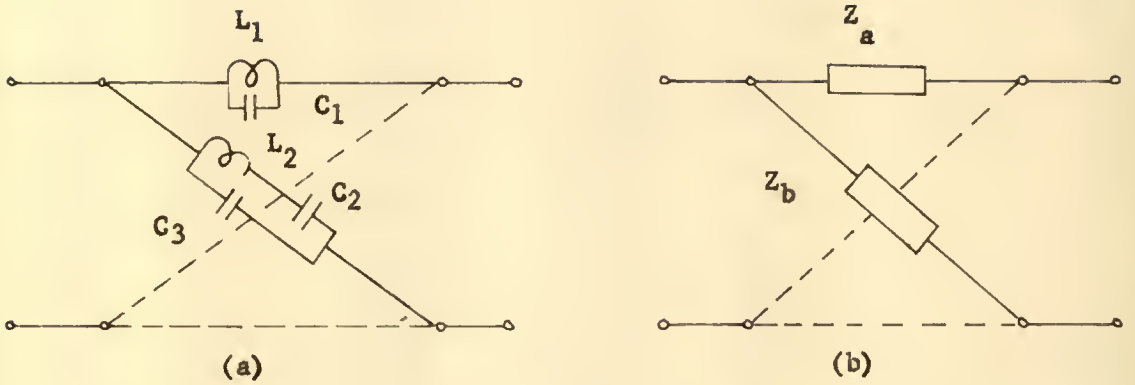

Fig. 3.3. Equivalent lattice of the ladder of Fig. 3.1.

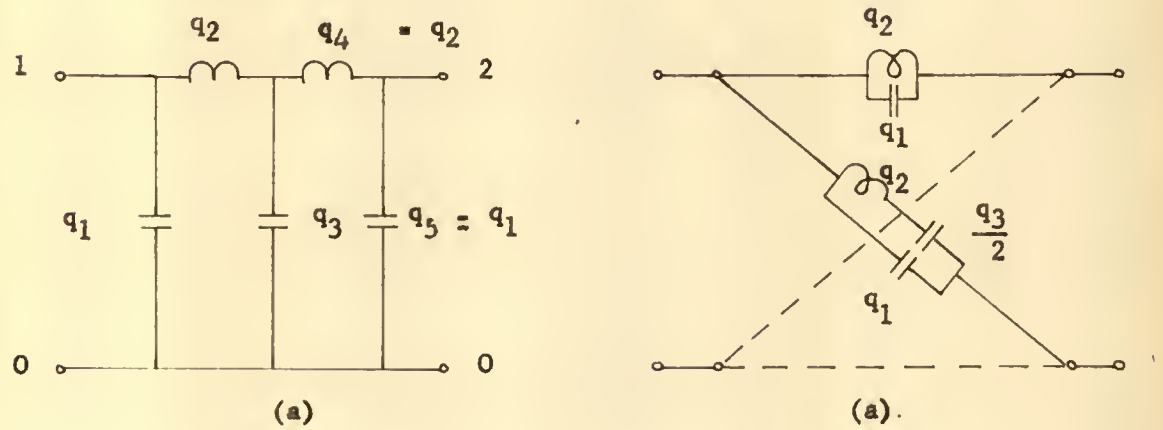

Fig. 3.4. A Butterworth and Tchebycheff type ladder filter and its equivalent lattice

The relation between the lattice and the ladder elements is as follows:

$$A_1 = \frac{q_1 - q_5}{q_4 a_4 - q_2 a_2} \tag{3.16}$$

$$A_2 = q_1 + q_2 a_2 A_1 \tag{3.17}$$

$$A_3 = \frac{1}{2}\left(\frac{q_3}{A_1} + q_2 a_2 + q_4 a_4\right) \tag{3.18}$$

$$A_4 = A_2 A_3 - q_2 a_2 q_4 a_4 A_1 \tag{3.19}$$

$$A_5 = \frac{1}{2}(q_1 + q_3 + q_5) \tag{3.20}$$

The insertion loss of the equivalent lattice of Fig. 3.3 is given by equation (3.1), where

$$E = \frac{B_1(\omega^4 - \omega^2 B_2 + B_3)}{\omega^4 B_4 - \omega^2 B_5 + 1} \tag{3.21}$$

$$B_1 = \frac{A_2 A_4}{A_1} \tag{3.22}$$

$$B_2 = \frac{A_1 A_4 + A_2 A_5 - A_3}{A_2 A_4} \tag{3.23}$$

$$B_3 = \frac{A_1 A_5 - 1}{A_2 A_4} \tag{3.24}$$

$$B_4 = \frac{1}{A_1}(A_2 A_3 - A_4) \tag{3.25}$$

$$B_5 = \frac{1}{A_1}(A_1 A_3 + A_2 - A_5) \tag{3.26}$$

The zeros and poles of the insertion loss are given by

the zeros and poles of equation (3.21), i.e.

$$\omega(\omega^4 - \omega^2 B_2 + B_3) = \left[\omega^4 - \omega^2(z_1^2 + z_2^2) + z_1^2 z_2^2\right]$$

$$\omega^4 B_4 - \omega^2 B_5 + 1 = \frac{\omega^4}{p_1^2 p_2} - \frac{\omega^2}{p_1^2 + p_2^2} + 1 \qquad (3.27)$$

where z_1, z_2 and p_1, p_2 are the frequencies at which the insertion loss is zero and infinite, respectively. It follows from equation (3.27)

$$B_2 = z_1^2 + z_2^2 \qquad (3.28)$$

$$B_3 = z_1^2 z_2^2 \qquad (3.29)$$

$$B_4 = \frac{1}{p_1^2 p_2^2} \qquad (3.31)$$

Equations (3.27) can be solved for the zeros and poles:

$$z_o = 0 \qquad (3.32)$$

$$z_{1,2}^2 = \frac{B_2}{2} \pm \left[\frac{B_2^2}{4} - B_3\right]^{\frac{1}{2}} \qquad (3.33)$$

$$p_o = \infty \qquad (3.34)$$

$$p_{1,2}^2 = \frac{B_5 \pm (B_5^2 - 4B_4)^{\frac{1}{2}}}{2B_4} \qquad (3.35)$$

3.3. Tchebycheff and Butterworth Filters Synthesized with Image Parameter Half-Sections

The Butterworth and Tchebycheff-type two-section filter is shown in Fig. 3.4(a) and its insertion loss characteristic is given by equation (3.1) with[17]

$$E = H\omega^5 \tag{3.36}$$

for the Butterworth filter, and

$$E = HT_5(\omega) \tag{3.37}$$

for the Tchebycheff filter. Here $T_5(\omega)$ is the Tchebycheff polynomial of order 5, which can be defined by

$$T_5(\omega) = \cos\ (5\cos^{-1}\omega\ ) \tag{3.38}*$$

$$0 \leq \omega \leq 1$$

The insertion loss zeros of the Butterworth filter, as seen from equation (3.36) are at $\omega = 0$; the Tchebycheff polynomial is zero when

$$5\cos^{-1} = \pi(i + \tfrac{1}{2})$$

$$i = 0, 1, \cdots 4$$

resulting in zero insertion loss at the following frequencies:

$$\begin{aligned} z_o &= 0 \\ z_1{}^2 &= \cos^2 \frac{\pi}{10} \\ z_2{}^2 &= \cos^2 \frac{3\pi}{10} \end{aligned} \tag{3.39}$$

---

*$T_n(x)$ can be defined in polynomial form as $T_n(z) = 2^{n-1}\left[x^n - nx^{n-2}/1!2^2 + n(n-3)x^{n-4}/2!2^4 - n(n-4)(n-5)x^{n-6}/3!2^6 + \cdots\right]$ where the summation is stopped when the exponents of x are negative. The form of (3.38) is convenient in that it exhibits the location of the zeros.

Equation (3.37) can be written, using equations (3.39),

$$E = \frac{H\omega\left(\omega^2 - \cos^2 \frac{\pi}{10}\right)\left(\omega^2 - \cos^2 \frac{3\pi}{10}\right)}{\left(1 - \cos^2 \frac{\pi}{10}\right)\left(1 - \cos^2 \frac{3\pi}{10}\right)} \tag{3.40}$$

For both, Butterworth and Tchebycheff, filter types $E = H$ when $\omega = 1$, giving (see Fig. 3.5 (a) and (b))

$$H^2 = 10^{0.1L_p} - 1 \tag{3.41}$$

where L_p is the maximum loss in passband in db.

It can be shown that Tchebycheff and Butterworth two-section filters possessing electrical symmetry have also geometrical symmetry, i.e. (Fig. 3.4 (a))

$$q_1 = q_5$$

$$q_2 = q_4 \tag{3.42}$$

hence the equivalent lattice to the ladder of Fig. 3.4 (a) can be easily found using Bartlett's bisection theorem.[18] The equivalent lattice is shown in Fig. 3.4 (b).

Comparison of Fig. 3.3 (a) with Fig. 3.4 (b) yields the following relations:

$$L_1 = L_2 = q_2$$

$$C_1 = C_3 = q_1 \tag{3.43}$$

$$C_2 = \frac{q_3}{2}$$

Inserting equations (3.43) into equations (3.11) to (3.15) gives

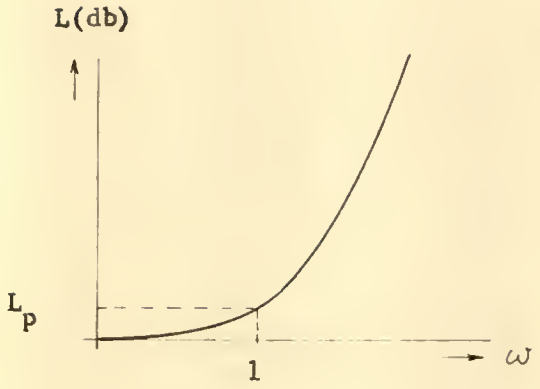

(a)

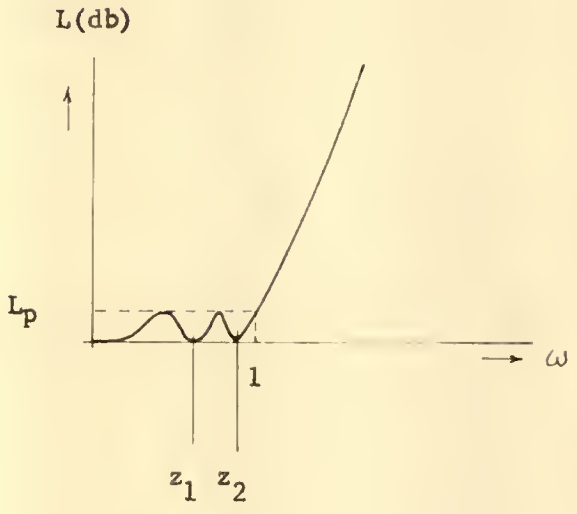

(b)

Fig. 3.5. Insertion loss characteristics for (a) Butterworth and (b) Tchebycheff two-section filters

$$A_1 = \frac{1}{q_2}$$

$$A_2 = q_1$$

$$A_3 = \frac{q_2 q_3}{2}$$

$$A_4 = \frac{q_1 q_2 q_3}{2}$$

$$A_5 = q_1 + \frac{q_3}{2} \qquad (3.44)$$

Equations (3.44) inserted in equations (3.22) to (3.26) give

$$B_1 = \frac{q_1{}^2 q_2{}^2 q_3}{2}$$

$$B_2 = \frac{2q_1 + 2q_3 - \frac{q_2 q_3}{q_1}}{q_1 q_2 q_3}$$

$$B_3 = \frac{2q_1 - 2q_2 + q_3}{q_1{}^2 q_2{}^2 q_3}$$

$$B_4 = B_5 = 0 \qquad (3.45)$$

Equations (3.2)to (3.8), with equations (3.42) and with $a_2 = a_4 = 0$ result in $m_{12} = m_{34} = 1$, $r_1 = r_4$ and $r_2 = r_3$, giving

$$q_1 = \frac{1}{r_1 \omega_c}$$

$$q_2 = \frac{r_1 + r_2}{\omega_c} \qquad (3.46)$$

$$q_3 = \frac{2}{r_2 \omega_c}$$

Substitution of equations (3.46) in (3.45) gives

$$B_1 = \frac{(r_1 + r_2)^2}{r_1^2 r_2 \omega_c^5}$$

$$B_2 = \omega_c^2\left(1 - r_1^2 + \frac{r_1}{r_1 + r_2}\right)$$

$$B_3 = \frac{\omega_c^4 r_1 (1 - r_1 r_2)}{r_1 + r_2} \qquad (3.47)$$

Finally, using equations (3.29) and (3.30) in equations (3.47) we get

$$z_1^2 + z_2^2 = \omega_c^2\left(1 - r_1^2 + \frac{r_1}{r_1 + r_2}\right)$$

$$z_1^2 z_2^2 = \frac{\omega_c^4 r_1 (1 - r_1 r_2)}{r_1 + r_2} \qquad (3.50)$$

The Butterworth Filter

The insertion loss zeros of the Butterworth filter are at zero frequency (i.e., at $\omega = 0$). Equations (3.50) then become (with $z_1 = z_2 = 0$)

$$0 = \omega_c^2\left(1 - r_1^2 + \frac{r_1}{r_1 + r_2}\right)$$

$$0 = \frac{\omega_c^4 r_1 (1 - r_1 r_2)}{r_1 + r_2} \qquad (3.51)$$

Solving equations (3.51) simultaneously we obtain

$$r_1 = \left[0.5 + (1.25)^{\frac{1}{2}}\right]^{\frac{1}{2}} = 1.27202$$

$$r_2 = \frac{1}{r_1} = 0.78615 \qquad (3.52)$$

Comparison of equation (3.21) with equation (3.36) shows that $B_1 = H$, hence from equations (3.41) and (3.47) we get

$$10^{0.1L_p} - 1 = \frac{(r_1 + r_2)^4}{r_1^4 r_2^2 \omega_c^{10}} \tag{3.53}$$

From equations (3.51) we get $r_1 + r_2 = r_1^3$, which inserted in (3.53) with $r_1 r_2 = 1$ from (3.52), gives

$$\omega_c = \frac{r_1}{H^{0.2}} = \frac{1.27202}{(10^{0.1L_p} - 1)^{0.1}} \tag{3.54}$$

The cut-off frequency ω_c is tabulated for values of L_p, the maximum attenuation in passband, from 0.1 db to 5.0 db in Table 1, and is plotted versus L_p in Fig. 3.6.

A two section Butterworth filter in terms of image parameter half-sections, with $L_p = 3$ db is shown in Fig. 3.7.*

The Tchebycheff Filter

With the insertion loss zeros of the Tchebycheff filter given by equations (3.39), equations (3.50) become

$$\cos^2 \frac{\pi}{10} + \cos^2 \frac{3\pi}{10} = \omega_c^2 \left(1 - r_1^2 + \frac{r_1}{r_1 + r_2}\right)$$

$$\cos^2 \frac{\pi}{10} \cos^2 \frac{3\pi}{10} = \frac{\omega_c^4 r_1 (1 - r_1 r_2)}{r_1 + r_2} \tag{3.55}$$

We also have from equations (3.21) and (3.40)

---

*For $L_p = 3$ db, $\omega_c = 1.272$ since $H = 1$ in equation (3.54).

TABLE 1

CUT-OFF FREQUENCY ω_c FOR THE BUTTERWORTH TWO-SECTION FILTER

L_p in db.

L_p	ω_c	L_p	ω_c	L_p	ω_c
0.1	1.8526	1.2	1.4263	3.2	1.2612
0.2	1.7265	1.4	1.4011	3.4	1.2503
0.3	1.6560	1.6	1.3792	3.6	1.2399
0.4	1.6071	1.8	1.3597	3.8	1.2300
0.5	1.5698	2.0	1.3421	4.0	1.2205
0.6	1.5396	2.2	1.3261	4.2	1.2113
0.7	1.5143	2.4	1.3113	4.4	1.2025
0.8	1.4925	2.6	1.2976	4.6	1.1939
0.9	1.4732	2.8	1.2847	4.8	1.1857
1.0	1.4560	3.0	1.2726	5.0	1.1776

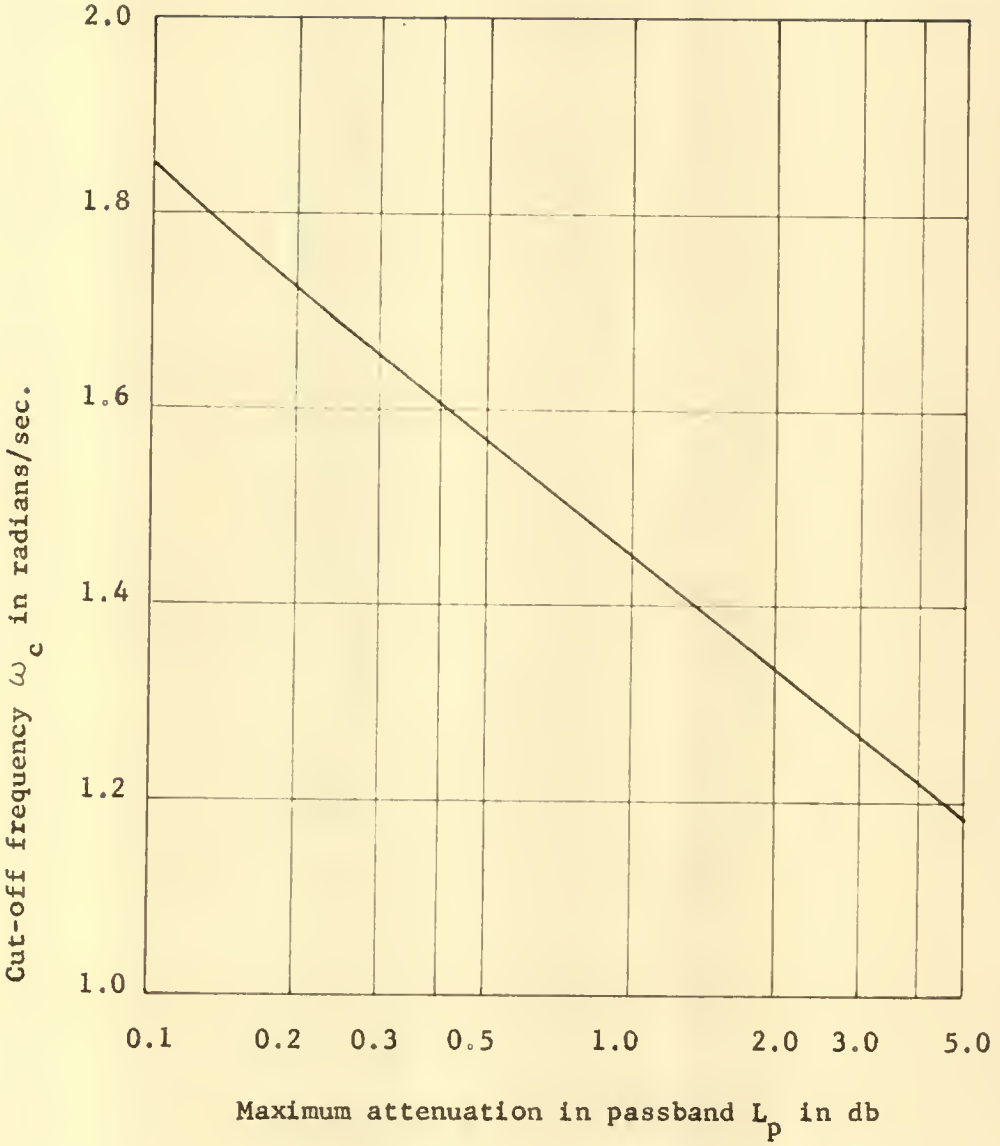

Fig. 3.6. Cut-off frequency of elementary building blocks versus maximum attenuation in passband for the design of filters with Butterworth characteristic

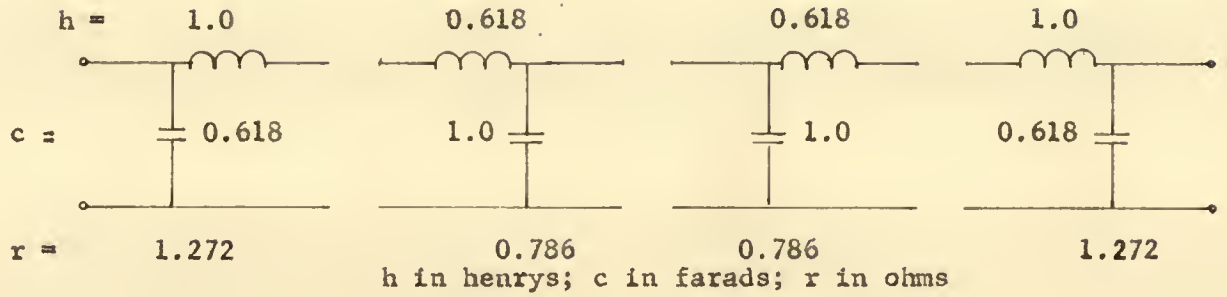

Fig. 3.7. A Butterworth filter in terms of elementary building blocks with $\omega_c = 1.272$ and $L_p = 3$ db

$$B_1 = \frac{H}{\sin^2 \frac{\pi}{10} \sin^2 \frac{3\pi}{10}}$$

with which (3.47) becomes

$$\frac{H}{\sin^2 \frac{\pi}{10} \sin^2 \frac{3\pi}{10}} = \frac{(r_1 + r_2)^2}{r_1^2 r_2 \omega_c^5} \tag{3.56}$$

Instead of attempting to solve directly equations (3.55) and (3.56) for ω_c, r_1 and r_2, it is more convenient to use equations (3.46) with the following equations derived by Belevitch[19]

$$\begin{aligned} q_1 &= \frac{2\sin \frac{\pi}{10}}{g} \\ q_2 &= \frac{2g\sin \frac{3\pi}{10}}{g^2 + \cos^2 \frac{3\pi}{10}} \\ q_3 &= \frac{2\left(g^2 + \cos^2 \frac{3\pi}{10}\right)}{g\left(g^2 + \cos^2 \frac{\pi}{10}\right)} \end{aligned} \tag{3.57}$$

where g is related to H by the transformation

$$\frac{1}{H} = \sinh 5x$$

$$g = \sinh x = \sinh\left(\frac{1}{5} \operatorname{arc\,sinh} \frac{1}{H}\right) \tag{3.58}$$

and H is given in terms of L_p, the maximum insertion loss in passband (which is here synonymous with the peak value of ripple in passband), by equation (3.41).

Equations (3.46) and (3.57) are readily solved for ω_c, r_1 and r_2, giving

$$\omega_c^2 = \frac{A + B}{4 \sin \frac{\pi}{10} \sin \frac{3\pi}{10}}$$

$$r_1^2 = \frac{g^2 \sin \frac{3\pi}{10}}{(A + B) \sin \frac{\pi}{10}}$$

$$r_2 = \frac{r_1 A}{B}$$

$$A = 2\left(g^2 + \cos^2 \frac{\pi}{10} \sin \frac{\pi}{10}\right)$$

$$B = g^2 + \cos^2 \frac{3\pi}{10} \qquad (3.59)$$

A tabulation of ω_c, r_1 and r_2 for values of L_p from 0.1 db to 5 db appears in Table 2.* A plot of ω_c, r_1 and r_2 from Table 2 versus L_p is shown in Fig. 3.8, and a Tchebycheff filter with $L_p = 1.5$ db in terms of image parameter half-sections is shown in Fig. 3.9.

3.4. The Elliptic Function Filter Synthesized with Image Parameter Half-Sections

The elliptic function type (often called equal ripple in passband and stop-band type) two-section filter which will be used

---

*The data in Table 2 are computed on the University of Florida IBM 650 computer from the equations (3.41), (3.58) and (3.59).

TABLE 2

IMAGE PARAMETER VALUES FOR THE TCHEBYCHEFF TWO-SECTION FILTER

L_p in db; r's in ohms

L_p	ω_c	r_1	r_2	r_2/r_1
0.1	1.1724	0.7428	0.8638	1.1613
0.2	1.1176	0.6680	0.8262	1.2368
0.3	1.0891	0.6197	0.7952	1.2831
0.4	1.0704	0.5837	0.7685	1.3166
0.5	1.0568	0.5547	0.7448	1.3427
0.6	1.0464	0.5304	0.7235	1.3640
0.7	1.0379	0.5094	0.7040	1.3820
0.8	1.0309	0.4909	0.6859	1.3974
0.9	1.0250	0.4743	0.6692	1.4109
1.0	1.0199	0.4593	0.6535	1.4228
1.2	1.0114	0.4329	0.6247	1.4431
1.4	1.0047	0.4102	0.5989	1.4599
1.6	0.9926	0.3903	0.5753	1.4741
1.8	0.9947	0.3725	0.5537	1.4862
2.0	0.9908	0.3565	0.5336	1.4968
2.2	0.9874	0.3419	0.5150	1.5061
2.4	0.9844	0.3285	0.4975	1.5144
2.6	0.9819	0.3161	0.4811	1.5218
2.8	0.9796	0.3046	0.4656	1.5284

TABLE 2 -- Continued

L_p	ω_c	r_1	r_2	r_2/r_1
3.0	0.9775	0.2939	0.4509	1.5344
3.2	0.9756	0.2838	0.4370	1.5399
3.4	0.9740	0.2743	0.4238	1.5449
3.6	0.9724	0.2653	0.4111	1.5495
3.8	0.9711	0.2569	0.3991	1.5537
4.0	0.9698	0.2488	0.3876	1.5575
4.2	0.9686	0.2412	0.3765	1.5611
4.4	0.9676	0.2339	0.3660	1.5644
4.6	0.9666	0.2270	0.3558	1.5675
4.8	0.9656	0.2203	0.3460	1.5704
5.0	0.9648	0.2140	0.3366	1.5730

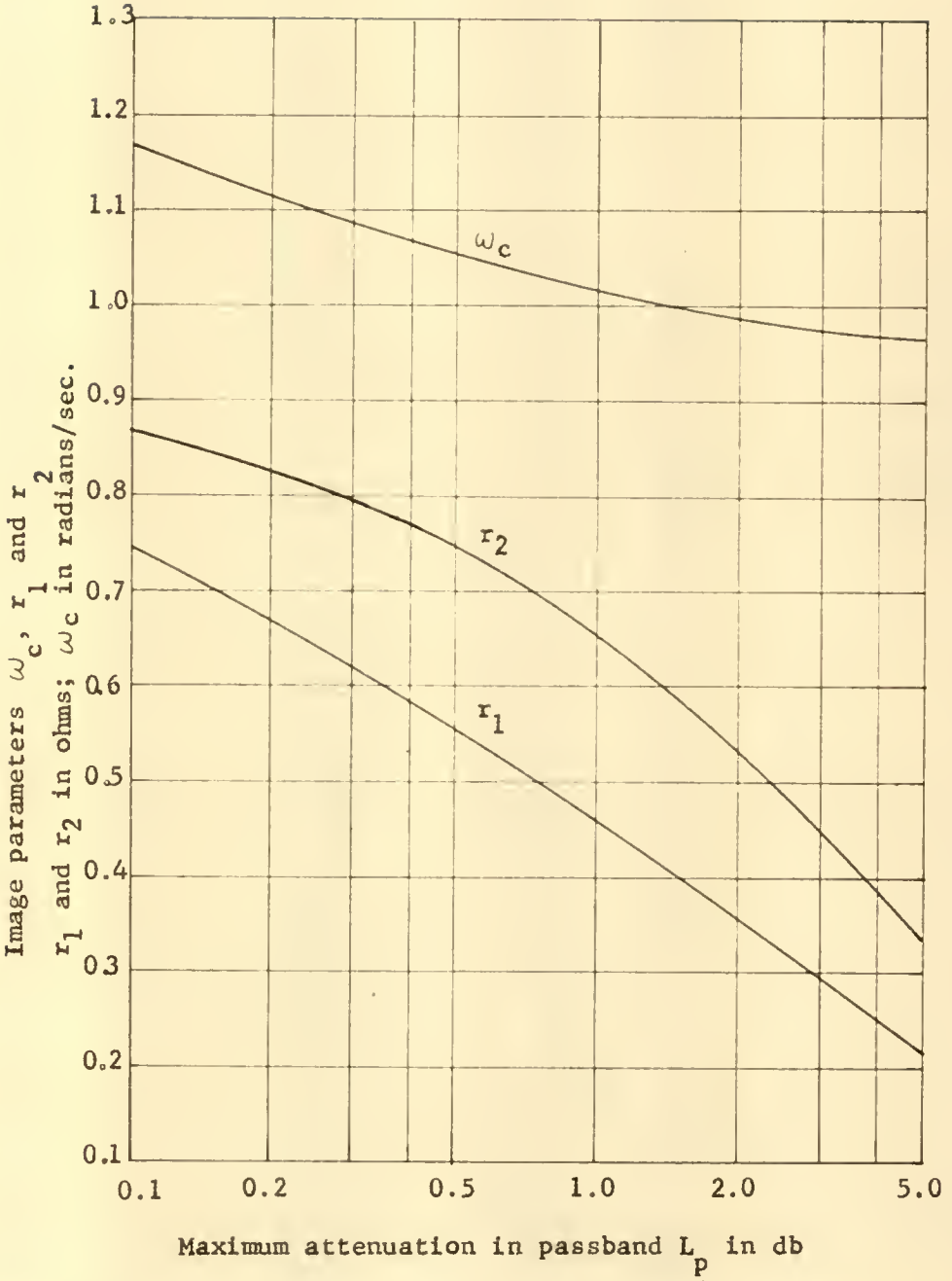

Fig. 3.8. Image parameters ω_c, r_1 and r_2 versus maximum ripple in passband for the design of filters with Tchebycheff characteristics

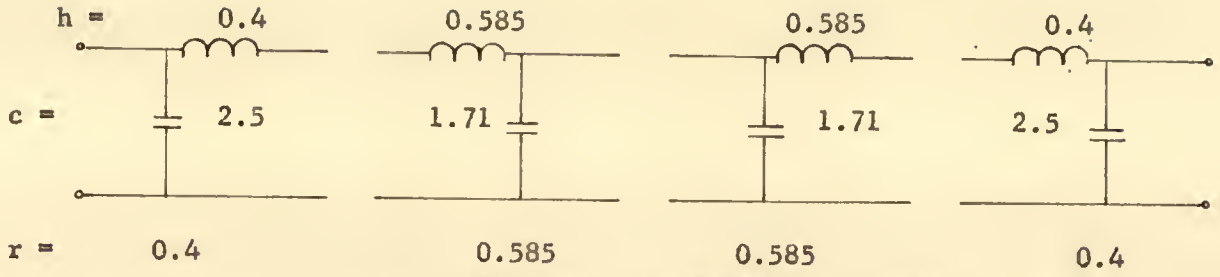

Fig. 3.9. A Tchebycheff filter with peak ripple in passband L_p = 1.5 db in terms of elementary building blocks with ω_c = 1.0

here is shown in Fig. 3.1,* and its insertion loss characteristic, Fig. 3.10, is given by equation (3.1) with[3]

$$E = \frac{H\omega(\omega^2 - z_1^2)(\omega^2 - z_2^2)}{(1 - \omega^2 z_1^2)(1 - \omega^2 z_2^2)} \tag{3.60}$$

The zeros of the insertion loss characteristic are given by

$$z_1 = k^{\frac{1}{2}} \, sn\left(\frac{2K}{5}, k\right)$$

$$z_2 = k^{\frac{1}{2}} \, sn\left(\frac{4K}{5}, k\right) \tag{3.61}$$

where sn denotes the elliptic sine, defined as[20, 21]

$$sn(u) = \sin \phi$$

$$u = F(k, \phi) = \int_0^{\phi} \frac{d\theta}{(1 - k^2 \sin^2 \theta)^{\frac{1}{2}}} \tag{3.62}$$

K denotes the complete elliptic integral of the first kind

$$K = K(k) = \int_0^{\frac{\pi}{2}} \frac{d\theta}{(1 - k^2 \sin^2 \theta)^{\frac{1}{2}}} \tag{3.63}$$

and k is the modulus of the elliptic sine.

The constant H is given by

$$H^4 = (10^{0.1L_p} - 1)(10^{0.1L_a} - 1) \tag{3.64}$$

---

*This is the special case of elliptic function filters in which all the poles are on the $j\omega$-axis, hence it can be realized with a ladder network that does not require mutual coupling.

where L_p is the maximum distortion in passband, and L_a is the minimum attenuation in stopband in decibels (see Fig. 3.10). L_p, L_a and k are related by[22]

$$L_a = 10 \log_{10} \left(1 + \frac{H^2}{\triangle^2}\right)$$

$$L_p = 10 \log_{10} \left(1 + H^2 \triangle^2\right)$$

$$\triangle = k^{\frac{5}{2}} \, sn^2 \left(\frac{K}{5}, k\right) sn^2 \left(\frac{3K}{5}, k\right) \qquad (3.65)$$

As can be seen from Fig. 3.10, the modulus k determines the width of the transition band (k is called the selectivity parameter),

$$k = \frac{\omega_p}{\omega_a} \qquad (3.66)$$

where ω_p is the upper frequency limite of the passband (or the effective cut-off frequency), and ω_a is the lower limit of the attenuation band.

When L_p is small and L_a large, which is the case for most filter requirements, the various parameters determining the response of an elliptic function type 2-section filter are related by the approximate equation

$$L_a \doteq 10 \log_{10} \left(10^{0.1 L_p} - 1\right) - 50 \log_{10} q - 12.041 \qquad (3.67)$$

where q is the elliptic modular function of k,* L_a and L_p are in

---

*The function log q is tabulated in most elliptic function tables, e.g., Ref. 21, pp. 49-51.

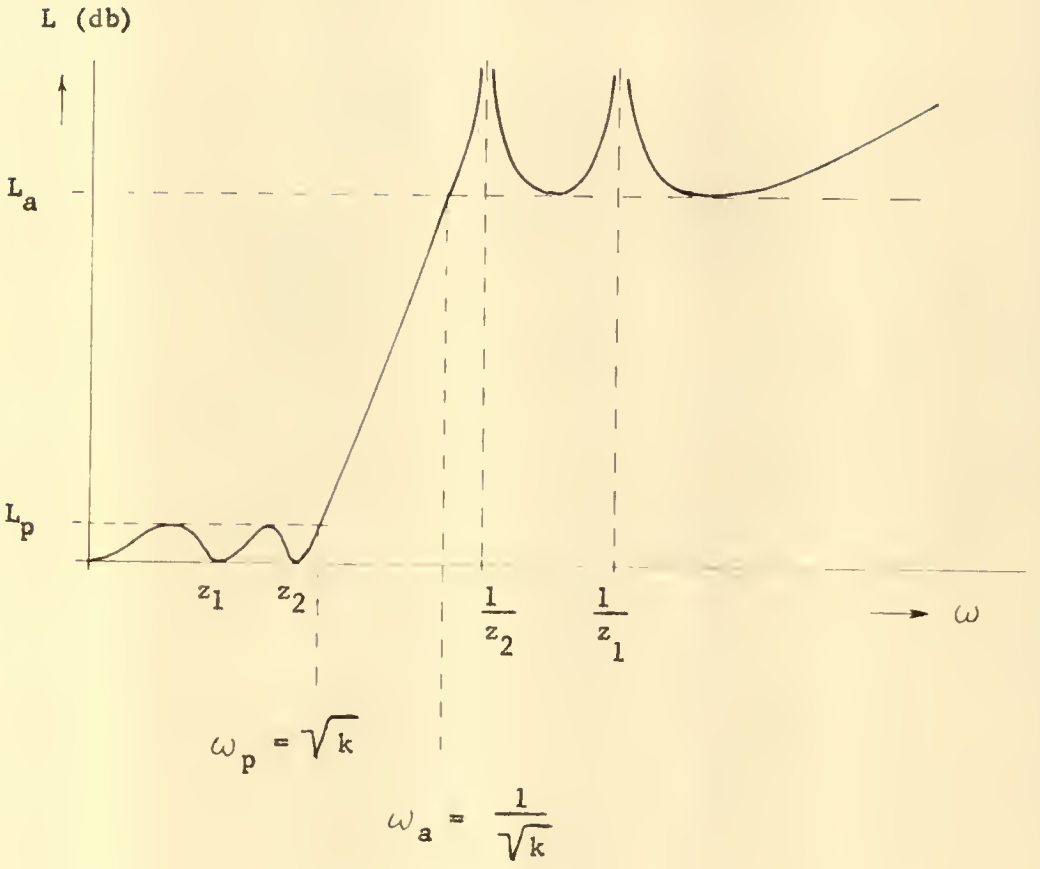

Fig. 3.10. Insertion loss characteristic of an elliptic function two-section filter

decibels. A plot of L_a versus k for $L_p = 0.1$ db is given in Fig. 3.11. Figure 3.12 shows the dependence of L_a on L_p for a given k.

In order to find relations between H, z_1, z_2 of equation (3.60) and the image parameters ω_c, r_1 to r_4, m_{12}, m_{34}, a procedure similar to one used in the previous section will be followed. The resulting algebraic manipulations are quite lengthy and will be omitted here. The following steps are carried out:

1. Equations (3.16) to (3.20) are inserted in equations (3.22) to (3.26), giving a set of equations, say Set I, relating B's with q's.

2. Equations (3.2) to (3.8) are inserted in Set I, giving a set of equations, say Set II, relating B's with the image parameters.

3. Equate Set II to corresponding equations (3.28) to (3.33), getting a set of equations, say Set III, relating the image parameters to the zeros and poles of the insertion loss function (3.60).

4. Solve equations Set III simultaneously for the image parameters in terms of zeros and poles of the insertion loss function.

Step 3 results in five non-linear equations in seven unknowns (the image parameters); two additional equations are obtained from the symmetry conditions which the ladder must satisfy, giving a total of seven independent equations. These seven equations do not lend themselves readily for use in Step 4,

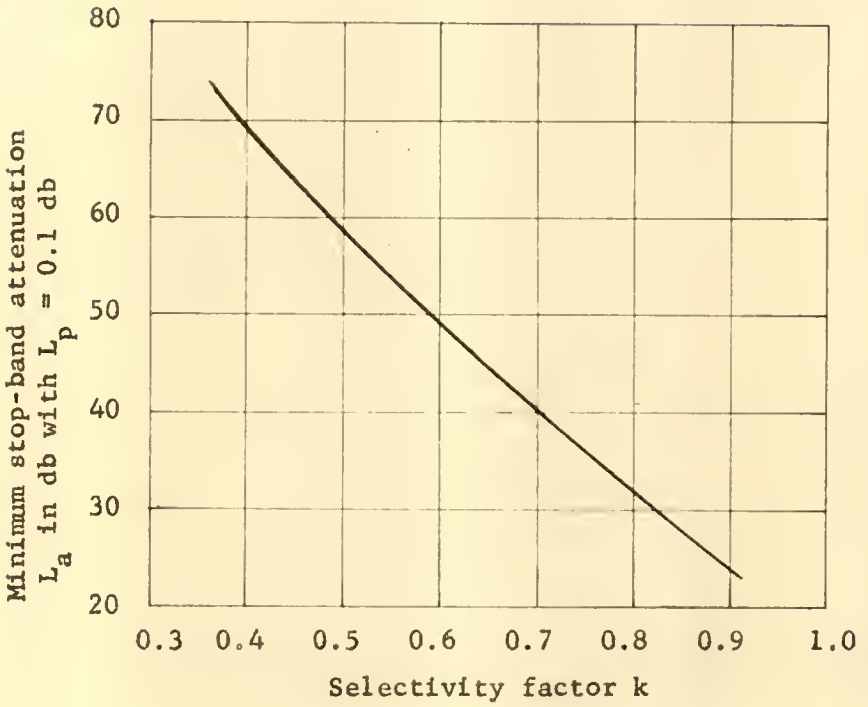

Fig. 3.11. Minimum stop-band attenuation L_a versus selectivity factor k for the two-section elliptic function filter

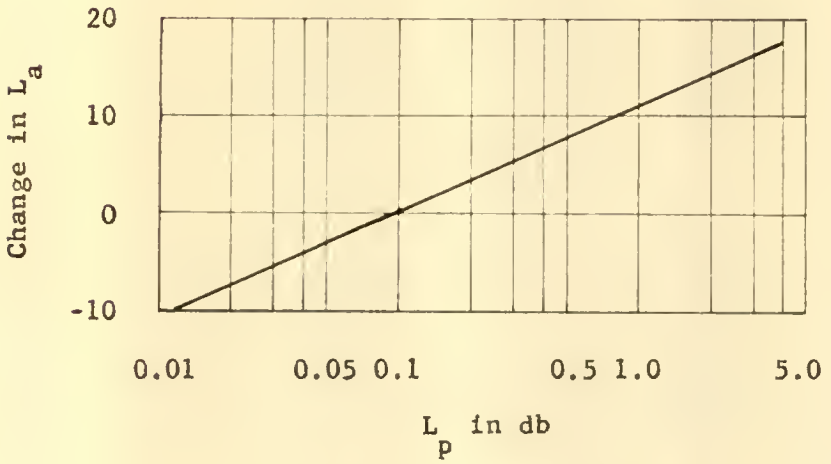

Fig. 3.12. Variation of minimum attenuation in stop-band with maximum ripple in passband

hence numerical values for the image parameters will be obtained using Method II (Chapter III).* Step 4 is carried out for a set of equations which are close approximations to those obtained in Step 3.

Following are the equations obtained in Step 3:

$$z_1^2 = \frac{1 - m_{12}^2}{\omega_c^2} \tag{3.68}$$

$$z_2^2 = \frac{1 - m_{34}^2}{\omega_c^2} \tag{3.69}$$

$$H = \frac{(m_{12}^2 - m_{34}^2)(1 + m_{12}m_{34}D)}{\omega_c^5(r_1m_{12} - r_4m_{34})} \tag{3.70}$$

$$\frac{z_1^2 + z_2^2}{\omega_c^2} = 1 + \frac{1 - r_1r_4(D + m_{12}m_{34})}{1 + m_{12}m_{34}D} \tag{3.71}$$

$$\frac{z_1^2 z_2^2}{\omega_c^4} = \frac{1 - r_1r_4D}{1 + m_{12}m_{34}D} \tag{3.72}$$

$$D = \frac{r_1m_{12} - r_4m_{34}}{r_4m_{12} - r_1m_{34}} \tag{3.73}$$

The equations obtained from symmetry conditions are:

$$r_1r_3 = r_2r_4 \tag{3.74}$$

---

*The numerical values appear in Table 3. They were obtained by analysis of synthesized elliptic function filters in terms of image parameter half-sections. For this purpose the synthesized filters published in Ref. 12 were used.

$$\frac{m_{12}m_{34}}{m_{12}^2 - m_{34}^2} = \frac{r_1 r_4 (r_1 - r_2)}{(r_4^2 - r_1^2)(r_1 + r_2)} \tag{3.75}$$

Equation (3.75) can be written as

$$\frac{r_2}{r_1} = \frac{(r_1 m_{12} - r_4 m_{34})(r_4 m_{12} + r_1 m_{34})}{(r_4 m_{12} - r_1 m_{34})(r_1 m_{12} + r_4 m_{34})} \tag{3.76}$$

to which a close approximation turns out to be

$$\frac{r_2}{r_1} \doteq \frac{r_1 m_{12} - r_4 m_{34}}{r_4 m_{12} - r_1 m_{34}} \tag{3.78}$$

with the assumption that*

$$1 \doteq \frac{r_4 m_{12} + r_1 m_{34}}{r_1 m_{12} + r_4 m_{34}} \tag{3.79}$$

With the approximation of equation (3.78) the following set of approximate relations may be obtained:**

$$H \doteq \frac{(m_{12} + m_{34})(1 + m_{12}m_{34})}{r_1 \omega_c^5} \tag{3.80}$$

$$z_1^2 + z_2^2 \doteq \omega_c^2 \left(1 - r_1 r_2 + \frac{1}{1 + m_{12}m_{34}}\right) \tag{3.81}$$

---

*This assumption is justified by the range of values of the r's and m's encountered in a great number of filters, as shown by the numerical data in Table 3. For most of the values computed, equation (3.79) turns out to be near 0.99.

**In addition to the approximation (3.78), there were also other approximations used which are implied in (3.78) and (3.79), e.g., $|r_1 - r_4| \ll 1$, arising from the fact that in most cases of interest $|m_{12} - m_{34}| \ll 1$.

$$z_1^2 z_2^2 \doteq \frac{r_1 \omega_c^4 (1 - r_1 r_3)}{r_1 + r_2 m_{12} m_{34}} \tag{3.82}$$

From (3.68) and (3.69) we have

$$m_{12} = (1 - \omega_c^2 z_1^2) \tag{3.83}$$

$$m_{34} = (1 - \omega_c^2 z_2^2) \tag{3.84}$$

Using equations (3.83) in (3.80), we may get

$$r_1 \doteq \frac{(m_{12} + m_{34})(1 + m_{12} m_{34})}{H \omega_c^5} \tag{3.85}$$

with which r_2 may be computed from (3.81)

$$r_2 \doteq \frac{1}{r_1} \left(\frac{m_{12} m_{34}}{1 + m_{12} m_{34}} - \frac{z_1^2 + z_2^2}{\omega_c^2} \right) \tag{3.86}$$

Equation (3.82) may be solved for r_3, using r_1 and r_2 from (3.85) and (3.86).

$$r_3 = \frac{1}{r_1} \left[1 - \frac{z_1^2 z_2^2 (r_1 + r_2 m_{12} m_{34})}{r_1 \omega_c^4} \right] \tag{3.87}$$

Using (3.85) to (3.87) in (3.74), we get

$$r_4 = \frac{r_1 r_3}{r_2} \tag{3.88}$$

The cut-off frequency ω_c in equations (3.83) to (3.87) may be computed from the approximation

$$\omega_c \doteq \frac{k^{\frac{1}{2}}}{0.982 + 0.01 \log_{10} L_p} \tag{3.89}*$$

*This equation was derived from the data in Table 3.

If more accurate results are desired, the r's may be re-evaluated by the following relations, using previously computed values on the right-hand side of the equations.

$$r_1 = \frac{(z_2^2 - z_1^2)(r_1 + r_2 m_{12} m_{34})}{H \omega_c^3 (r_1 m_{12} - r_4 m_{34})} \tag{3.90}$$

$$r_3 = \frac{1 - (\frac{z_1^2 + z_2^2}{\omega_c^2} - 1)(1 + \frac{r_2 m_{12} m_{34}}{r_1})}{r_1 (1 + \frac{r_1 m_{12} m_{34}}{r_2})} \tag{3.91}$$

$$r_4 = \frac{r_3 m_{12} m_{34}}{\frac{(1 - r_1 r_3)\omega_c^4}{z_1^2 z_2^2} - 1} \tag{3.92}$$

With r_1, r_3 and r_4 from above and r_2 from (3.74), ω_c can be recomputed from

$$\omega_c^2 = \frac{R(z_2^2 - z_1^2)}{m_1 m_2} \tag{3.93}$$

where R is the right-hand side of equation (3.75).*

A tabulation of r_1 to r_4, m_{12}, m_{34} and ω_c appears in Table 3 (see footnote on page 54). A plot of the r's versus L_p is shown in Fig. 3.13.

---

*The difference between the recomputed values and the first values of the r's and ω_c is an indication of the accuracy of the results. For greater accuracy, the image parameters may be computed by an iterative procedure using equations (3.68) to (3.75).

TABLE 3

IMAGE PARAMETER VALUES FOR THE ELLIPTIC-FUNCTION TYPE TWO-SECTION FILTER

L_a in db, r's in ohms

L_a	k	r_1	r_2	r_3	r_4	m_{12}	m_{34}	ω_c
				L_p = 0.1 db				
35	0.764	0.744	0.823	0.810	0.700	0.818	0.552	0.983
40	0.707	0.746	0.836	0.822	0.734	0.854	0.637	0.952
45	0.649	0.748	0.843	0.832	0.738	0.881	0.703	0.919
50	0.591	0.752	0.750	0.973	0.745	0.903	0.759	0.884
55	0.537	0.745	0.852	0.844	0.738	0.922	0.804	0.847
60	0.488	0.740	0.856	0.849	0.734	0.937	0.840	0.809
65	0.442	0.739	0.858	0.853	0.734	0.950	0.871	0.771
70	0.398	0.741	0.860	0.856	0.737	0.960	0.896	0.735
				L_p = 0.5 db				
35	0.843	0.530	0.739	0.693	0.495	0.791	0.526	0.954
40	0.787	0.532	0.745	0.707	0.503	0.831	0.601	0.927
45	0.731	0.539	0.749	0.718	0.518	0.864	0.674	0.895
50	0.675	0.544	0.747	0.719	0.531	0.891	0.733	0.860
55	0.618	0.557	0.757	0.716	0.556	0.912	0.784	0.824
60	0.561	0.550	0.746	0.733	0.540	0.929	0.824	0.789
65	0.510	0.550	0.745	0.735	0.542	0.943	0.857	0.753
70	0.462	0.555	0.753	0.744	0.548	0.954	0.883	0.720

TABLE 3 -- Continued

L_a	k	r_1	r_2	r_3	r_4	m	m	ω_c
				L_p = 1.0 db				
35	0.874	0.426	0.661	0.598	0.388	0.772	0.502	0.949
40	0.822	0.430	0.660	0.613	0.400	0.815	0.580	0.923
45	0.803	0.443	0.670	0.633	0.419	0.850	0.649	0.895
50	0.711	0.447	0.667	0.640	0.429	0.881	0.715	0.859
55	0.654	0.449	0.661	0.641	0.435	0.904	0.768	0.824
60	0.597	0.451	0.657	0.642	0.441	0.923	0.812	0.788
65	0.543	0.452	0.653	0.642	0.443	0.938	0.847	0.752
70	0.491	0.452	0.655	0.650	0.443	0.951	0.875	0.718

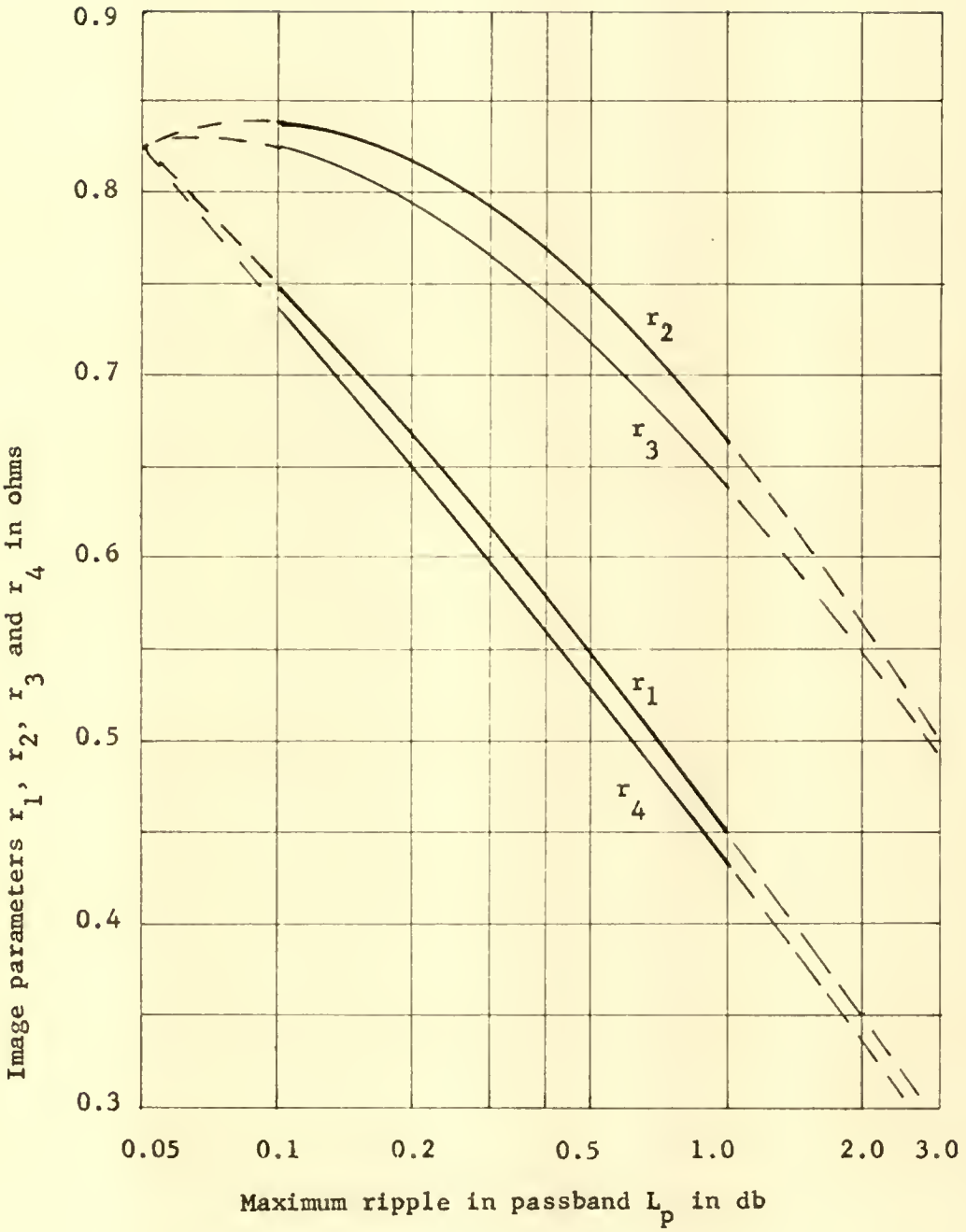

Fig. 3.13. Image parameters r_1, r_2, r_3 and r_4 for k = 0.7 versus maximum ripple in passband for the design of elliptic function filters

CHAPTER IV

ANALYSIS OF RESULTS AND CONCLUSIONS

4.1. Analysis of Obtained Data

It can be seen from the data in Table 3 that the r's show very little dependence on the selectivity factor k for quite a large range of values of k (the maximum change in the r's for a constant value of ripple in passband is about 5 per cent for values of k in an interval of about 0.4 to 0.8). If the Tchebycheff filter is considered as a limiting case of an elliptic function filter in which $k \to 0$,* i.e., all the poles of which were moved to infinity without appreciably changing the location of the zeros, we may use the data in Table 2 for getting the r's for the lower limit of $k = 0$. It is seen that these r-values differ little from the corresponding r's (i.e., r's for the same ripple in passband) of the elliptic-function filter.

The r's do, however, show strong dependence on the amount of ripple in passband L_p.

Defining mismatch constants as

---

*This is true only in an approximate sense, when the curve on which the zeros of the elliptic function insertion power-ratio are located (in complex frequency phase) approximates an ellipse. The distribution of the zeros on an ellipse-like curve is found in most practical cases of elliptic function type ladder filters without mutual coupling.

$$u_t = \frac{r_t}{r_1} = \frac{1}{r_1} \qquad (4.1)^*$$

$$u_1 = \frac{r_1}{r_2} \qquad (4.2)$$

$$u_2 = \frac{r_2}{r_3} \qquad (4.3)$$

it is seen that as the ripple in passband L_p increases, u_t increases, u_1 decreases, and u_2 shows very little dependence on L_p.

The effect of increasing u_t and decreasing u_1 may be visualized in complex frequency plane as moving the zeros of the insertion voltage ratio toward the j-ω axis, i.e., the effect is similar to that of predistortion. This suggests that in networks with incidental dissipation, a compensation for losses similar to predistortion may be achieved by an increase of u_t and a decrease of u_1, in amounts depending on the amount of losses (i.e., Q or d as defined in 2.4) in the components. A larger change in u_t and u_1 will be required for components with higher losses.

As seen from equation (3.89), the cut-off frequency ω_c varies predominantly with the square root of k, i.e., with the effective cut-off frequency ω_p (see Fig. 3.10).

The m's are functions of ω_c and the location of the poles

---

*r_t is the terminating resistance, which is equal to 1 ohm in our analysis.

of the insertion loss function $E(\omega)$, equation (3.83) and (3.84).* Since the location of the poles depends on the selectivity parameter k only, as seen from equation (3.61) and (3.63), and since ω_c depends on k predominantly, the m's depend mostly on k and very little on the amount of ripple in passband L_p.

4.2. Suggested Modification of Zobel Designs with the View of Obtaining More Efficient** Filters

The method of designing a Zobel filter to satisfy given insertion loss requirements has been appropriately called the cut-and-try method. One reason for this is the fact that the performance of a filter (i.e., its attenuation and phase-shift when inserted between generator and load) is only approximately given by its image attenuation and phase. This approximation is fairly good in the attenuation band, but is very poor in the pass-band.

The labor required to design a Zobel filter that approximately meets given requirements is usually very small. A commonly employed method of obtaining a filter which satisfies given requirements may be described in the following general steps:

1. Design a Zobel filter which approximately satisfies insertion loss requirements.

---

*In these equations the zeros z_1 and z_2, rather than the poles, appear. However, the poles are located inversely with respect to the zeros in the elliptic function filter, as seen from equation (3.60).

**The term "efficient" is used here in the sense of high contribution to filtering action for each component.

2. Build a model filter according to design of Step 1.

3. Test the model of Step 2, establishing the difference between its performance and the requirements.

4. Dictated by the results of Step 3, make corrective changes in the design of Step 1, aiming at eliminating the difference between the filter performance and the requirements.

5. Repeat Steps 2, 3 and 4 until the aim of Step 4 is reached.

It should be pointed out here that the cost (in terms of effort or dollars) of arriving at a satisfactory design using the above method is usually smaller than the cost of a design carried out by modern network-design techniques (i.e., by insertion parameter synthesis, leading to a satisfactory design in a more direct way).* This may partially account for the fact that Zobel designs are still so widely employed, although the modern techniques (in existence now for about twenty years) are known to produce better, often more economical, filters.

It is in general easier to correct the performance of a filter (Step 4) in attenuation band than in passband. In fact, unwanted distortion in passband may sometimes be eliminated only by adding components to the filter (e.g., m-derived terminal half-sections), or by using an additional network (an attenuation equalizer). This is due to the pattern of distortion in passband inherent in

---

*This is particularly so if the designer has reasonable ability to predict the effects of changes in design (i.e., changes of Step 4).

Zobel filters, as shown in Fig. 4.1.

The insertion loss in passband of Zobel filters with equal image impedances Z_I at both terminations, inserted between equal resistances R_t, is given by[24]

$$L = 10 \log_{10} \left[1 + \frac{1}{4} \left(\frac{Z_I}{R_t} - \frac{R_t}{Z_I} \right) \sin^2 B \right]$$

where B is the total phase shift through the filter. The envelope of the insertion loss in passband is

$$L_{env} = 20 \log_{10} \left[\frac{1}{2} \left(\frac{Z_I}{R_t} - \frac{R_t}{Z_I} \right) \right]$$

Since the image impedance Z_I is continuous in passband and becomes zero (or infinite) at the cut-off frequency ω_c in a manner indicated by Figs. 2.2 and 2.3, termination of the filter by a constant resistance R_t results in an insertion loss envelope in passband which increases near the cut-off frequency ω_c, as indicated in Fig. 4.1.

Most filter requirements allow a certain amount of maximum distortion in passband. Fig. 4.2 shows a typical insertion loss requirement; any insertion loss curve laying in the shaded area would satisfy the requirements. The curve shown may be considered typical for an efficient* one-section filter.

---

*In general, the number of components needed in a filter increases with increased selectivity $k = \omega_p/\omega_a$, with increased minimum loss in attenuation band L_a and L_h, and with decreased maximum distortion in passband L_p. The curve shown utilizes the limits of the requirements in a fashion which could lead to a filter with fewest components.

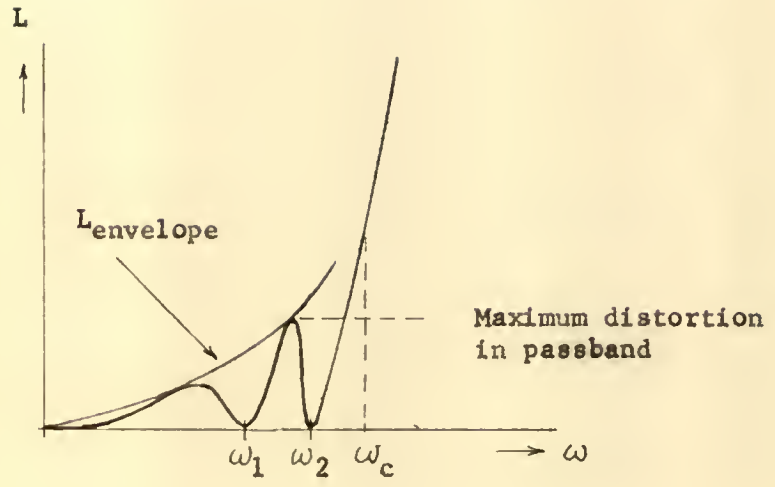

Fig. 4.1. Typical insertion loss characteristic in passband for a Zobel filter

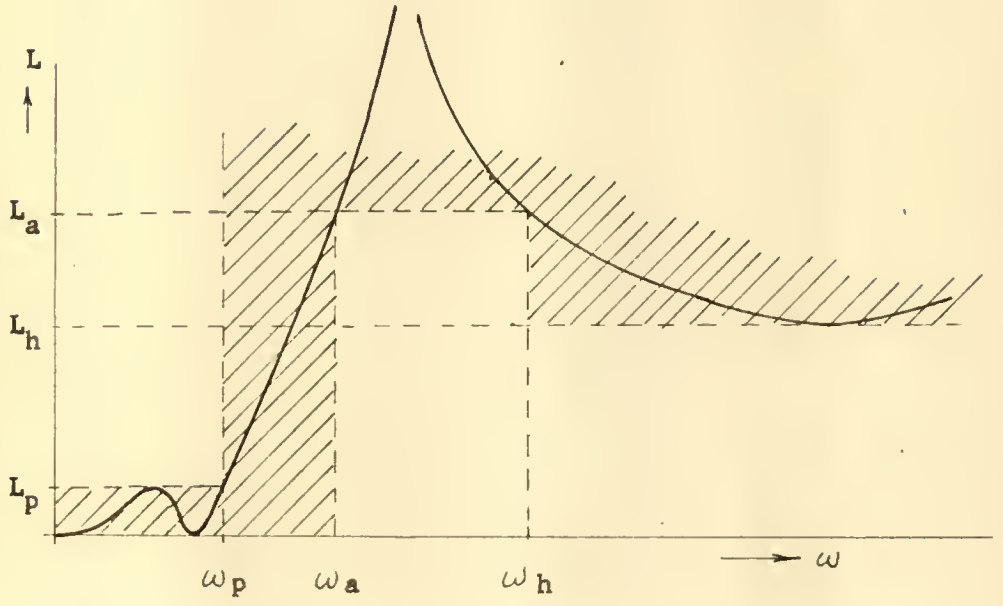

Fig. 4.2. Typical insertion loss requirement (straight lines) and a possible insertion loss characteristic which satisfies it

In case of the Tchebycheff and elliptic function filters, utilization of the maximum allowable distortion in passband, i.e., designing a filter that has this maximum distortion in passband, leads to meeting the requirements with a filter having a minimum number of elements. Since the Tchebycheff and elliptic function filters can be designed to produce a predetermined amount of maximum distortion in passband (in contrast to the Zobel filter, in design stage of which there is no provision for obtaining a certain predetermined amount of distortion in passband), these filters can be designed to satisfy given requirements with a minimum number of components.*

In case of the Zobel filter, the amount of distortion in passband can be controlled by mismatch at the filter terminals, i.e., by choice of the value for R_t, within a relatively narrow range only. In general, a Zobel design is termed successful if the filter satisfies the requirements in attenuation band, and turns out to have passband distortion which is below (or equal) the specified maximum allowable distortion.

---

*Tuttle[25] showed in a comparison of the performance of Butterworth, inverted Tchebycheff, elliptic-function, constant-k and m-derived Zobel filters that the Zobel filter was inferior to the elliptic function type only. However, a comparison of a constant-k Zobel filter with a Tchebycheff filter should prove that the latter has superior performance for the same number of elements.

If the requirement calls for a very small distortion in passband (in the 0.01 db. range), the usual way to obtain it with a Zobel design is by the use of m-derived terminating half-sections, the image impedance of which (see Fig. 2.3) has less variation over an appreciable portion of the passband than the prototype (constant-k) image impedance, Fig. 2.2. This then results in smaller passband distortion due to better matching at the terminations, the price for which is an increased number of elements (above the number necessary to produce a given selectivity and discrimination) required in the m-derived terminations.*

If the allowable distortion in passband is high (in the 1 db. range), the Zobel design can take little advantage of it since at best the maximum distortion will be reached at one point in the passband, as indicated in Fig. 4.1.**

From this it may be concluded that in order to make a Zobel filter more efficient (comparable to a Tchebycheff or elliptic function filter), some means of

1. Controlling the amount of distortion in passband

2. Achieving equal (or approximately equal) maximum ripple in passband should be included in the design procedure.

---

*In some cases additional attenuation equalizing networks are used instead of, or for severe requirements, with the m-derived terminations.

**An efficient (in terms of the number of components) design results when the maximum allowable distortion in passband is reached a maximum possible number of times[3] as in the case of the Tchebycheff and elliptic function filters.

It was shown in Article 4.1 that for the elliptic function filter the values of the r's are determined mainly by the ripple in passband, whereas all the other parameters (ω_c and the m's) depend mainly on the selectivity k. This means that the main effect of a change in the r's will be a change in passband distortion. There is a certain relation between the changes in the individual r's which results in an equal ripple of a certain magnitude. These changes depend only little on the position of the poles (i.e., ω_c and m) in the attenuation band.

From the above reasoning the following may be concluded:

Given a Zobel filter designed with any image parameters (ω_c, r_o and m's), the amount of distortion in passband may be controlled by changes in the impedance levels (i.e., in the r's) of its half-sections. In particular, for a Zobel filter consisting of m-derived sections, an approximately equal ripple in passband of magnitude L_p will be obtained if the values of the r's are made equal to the corresponding r's of the elliptic-function type filter having the same amount of ripple in passband and approximately the same selectivity k; for a Zobel filter consisting of constant-k sections, an approximation to equal ripples of magnitude L_p will be achieved by letting the r's of the Zobel filter assume the values of corresponding r's of the Tchebycheff filter with a passband distortion of L_p.

Since, as it was pointed out in Article 4.1 (p. 61), the

r-values of a Tchebycheff filter having a certain amount of passband ripple L_p differ only slightly from corresponding r-values of an elliptic-function type filter having the same passband ripple L_p, it appears that:

> Making the impedance levels (the r's) of the half-sections of any Zobel filter (i.e., consisting of m-derived or constant-k sections and having any selectivity) equal to the corresponding r's of a Tchebycheff filter with passband ripples of magnitude L_p, will result in the insertion loss of the thusly modified Zobel filter to have approximately equal passband ripples of the same magnitude L_p.

4.3. Limits of Improvement of a Zobel Filter

There are many ways by which one may carry out the details of a Zobel filter design as outlined in Step 1, Article 4.2. These will in general depend to some extent on the type of the insertion loss requirements. Since this subject is well covered in literature,[15, 16, 26] it will not be repeated here.

For the purpose of this article it will be assumed that Step 1 has been carried out for two types of insertion loss requirements shown by the straight lines in Fig. 4.3 (a) and (b),* and that the resulting Zobel filters have an insertion loss as shown by the solid curves in Fig. 4.3.

If now the half-sections of these filters are mismatched as

---

*These two types of requirements are among the most commonly encountered in practice.

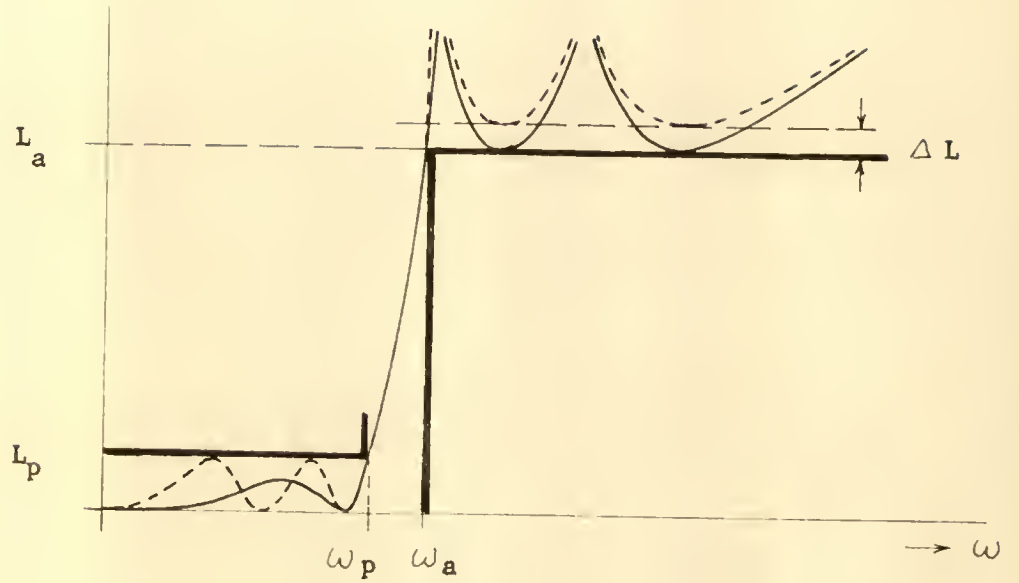

(a)

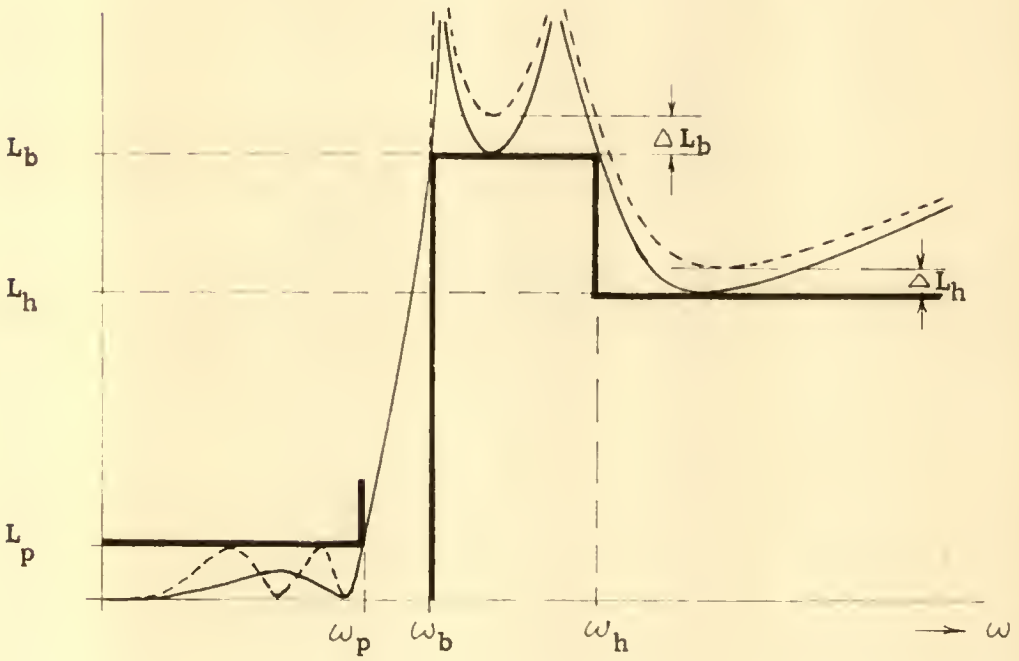

(b)

Fig. 4.3. Two types of insertion loss requirements and possible filter characteristics

outlined in Article 4.2, an insertion loss indicated by the dotted curves will be obtained. The question arises, how much of an improvement in performance of these filters may be expected from this mismatch?

In the case of the filter in Fig. 4.3 (a), the answer comes from the fact that the new insertion loss (dashed curve) can be at best as good as the insertion loss of an elliptic function type filter with passband ripple L_p and selectivity $k = \omega_p / \omega_a$. The minimum insertion loss in attenuation band L_{ae} of such a filter is given by equation (3.65) or (3.67), or can be found from the curve in Fig. 3.11. Hence, at best, the improved performance of a modified Zobel filter will be an increase of the minimum insertion loss in stop-band by*

$$\Delta L = L_{ae} - L_a \tag{4.4}$$

In the case of the filter in Fig. 4.3 (b), it is convenient to use a transformation[26] which will express the performance of the filter in terms of a performance as in Fig. 4.3 (a). It turns out that the minimum attenuation L_{be} in the frequency range ω_b to ω_h is approximately the same as the minimum attenuation L_{be} for

---

*If the Zobel filter (before modification) had equal minima of insertion loss in passband, as indicated by the solid curves in Fig. 4.3, the minima will not, in general, be equal after the modification, i.e., after mismatching the half-sections. For most cases occurring in practice, however, the difference in the minima will be small and can easily be corrected by a small change in the m-values, the effect of which on the passband ripple is neglibible.

a filter as Fig. 4.3 (a) with a selectivity of

$$k = \frac{\omega_p}{\omega_b} \left[\frac{1 - \left(\frac{\omega_b}{\omega_h}\right)^2}{1 - \left(\frac{\omega_p}{\omega_h}\right)^2} \right]^{\frac{1}{2}} \qquad (4.5)^*$$

L_{be} may be determined in the same manner as L_{ae} for the previous case, giving the maximum possible improvement as

$$\Delta L_b = L_{be} - L_b \qquad (4.6)$$

4.4. Summary and Conclusions

A method of synthesis of ladder networks was investigated with which conventional ladder networks may be obtained by proper choice of parameters of elementary building blocks.

---

*The frequency scale in Fig. 4.3 (b) is transformed to an m-scale by the relation $m = (1 - \omega_p^2/\omega^2)^{1/2}$, hence $m = 0$ corresponds to ω_p, $m = 1$ corresponds to $\omega = \infty$, m_b and m_h correspond to ω_b and ω_h, respectively. Multiplication of the m-scale by a factor $1/m_h$ introduces a new scale, say m' scale, in which $m' = 0$ corresponds to ω_p, $m' = 1$ corresponds to ω_h, and $m_b' = m_b/m_h$ corresponds to ω_b. An inverse transformation of m', i.e., $\omega' = \omega_p/(1 - m'^2)^{1/2}$, results in a frequency scale ω' which is infinite at ω_h, giving an insertion loss requirement with equal minimum from ω_b' (corresponding to ω_b) to $\omega' = \infty$. The selectivity of the transformed requirement is $k = \omega_p'/\omega_b'$, giving (4.5) upon substitution of $\omega_p' = \omega_p$ and $\omega_b' = \omega_p/(1 - m_b')^{1/2}$.

These parameters were determined for three types of two-section filters having desirable insertion loss characteristics.

As a result of analysis of the obtained parameter values, a method for improving Zobel filters was suggested.

The design of a two-section Butterworth filter can be quite simply accomplished with image parameter half-sections having a constant amount of impedance mismatch given by equation (3.52) and a cut-off frequency ω_c given by equation (3.54) or Fig. 3.6. The impedance levels of the half-sections, r_1 and r_2, are constant, i.e., independent of any design parameter; the cut-off frequency ω_c is a function of the maximum distortion in passband only, as given by equation (3.54).*

The design of two-section Tchebycheff filters may be as easily performed using equation (3.58) and (3.59), or the graphs in Fig. 3.8.**

---

*The ctt-off frequency ω_c is not a critical design parameter for constant -k type low-pass and high-pass filter types, i.e., it has no effect on the shape of the response curve. A change in the cut-off frequency amounts to a linear transformation of the frequency scale of the insertion loss versus frequency curve.

**Butterworth and Tchebycheff filters with lossless elements can be designed with not much effort using already developed formulae for element values (i.e., without going through the actual synthesis from the insertion loss function). The engineering value of our approach is in the simplifications resulting from its application to lossy networks, for which no explicit formulae for circuit element values are available at the present.

Computation of the element values by slide rule gives sufficient accuracy for commonly encountered tolerances in manufacturing of the components.*

A two-section filter of the elliptic-function type can be designed using either the equations (3.83) to (3.89),** or the graphs in Fig. 3.13 with equations (3.83), (3.84), (3.89) and (3.74); use of the graphs is simpler but more restricted in the range of application.

---

*A manufacturing tolerance in component values of $\pm$ 1.0 per cent to $\pm$ 2 per cent is quite common for capacitors in the range of approximately 100 $\mu\mu$f to 0.2 μf and for inductors in the range of approximately 1 mh to 50 hy.

**The values of the zeros, equation (3.61), can be found from many elliptic function tables, e.g., Ref. 21; they are tabulated for use in elliptic-function filter design in Ref. 23.

REFERENCES

1. O. J. Zobel, "Theory and Design of Uniform and Composite Electric Wave Filters," B.S.T.J., 2 (1923) pp. 1-46, and "Transmission Characteristics of Electric Wave Filters," B.S.T.J., 3 (1924), pp. 567-620.

2. M. I. Pupin,"Wave Propagation Over Non-Uniform Cables and Long Distance Air Lines," Trans. A.I.E.E., 17,(1900), pp. 445-507.

   G. A. Campbell, "On Loaded Lines in Telephonic Transmission," Phil. Mag., 5,(1903), pp. 313-330, and "Physical Theory of the Electric Wave Filter," B.S.T.J., 1 (1922), pp. 1-32.

   G. A. Campbell and R. M. Foster, "Maximum Output Networks for Telephone Substation and Repeater Circuits," Trans. A.I.E.E. vol. 39 (1920), pp. 231-280.

3. S. Darlington, "Synthesis of Reactance 4 - Poles," J. Math. Phys., vol. 18 (1939), pp. 257-353.

4. W. Cauer, Theorie der linearen Wechselstromschaltungen, Akademische Verlag, Berlin, Germany (1954), 2nd ed.

   H. Piloty, "Weichenfilter," Zeitschrift für Telegraphen und Fernsprechtechnik, vol. 28 (1939), pp. 291-298, 333-344, and "Wellenfilter, Insbesondere symmetrische und antimetrische mit vorgeschriebenem Betriebsverhalten," Zeitschrift für Telegraphen und Fernsprechtechnik, vol. 28, No. 10 (1939) pp. 363-375.

5. V. Belevitch, "Recent Developments in Filter Theory," IRE Transactions on Circuit Theory, vol. CT-5 (Dec. 1958) pp. 236-252.

6. T. Laurent, "Allgemeine physicalische Zusammenhänge bei Filterketten," Arch. d. El. Ü. B. 12, H.1 (Jan. 1958) pp. 1-8, and "Echostatanpassung, eiee neue Methode zur Anpassung von Spiegelparameterfiltern," Arch. d. El. Ü. B. 13, H. 3 (March 1959) pp. 132-140.

7. R. O. Rowlands, "Composite Ladder Filters," Wireless Engineer, vol. 29 (Feb. 1952) pp. 51.

8. J. E. Colin, "Two-Branch Filter Structures with Three Cut-Off Frequencies," Cables & Transmission, vol. 11 (July 1957) pp. 179-217.

9. W. Saraga, "Insertion Parameter Filters," TMC Technical J., vol. 2 (March 1951), pp. 25-36.

10. A. J. Grossman, "Synthesis of Tshebycheff Parameter Symmetrical Filters," Proc. IRE, vol. 45 (April 1957) pp. 454-473.

10. E. Green, Amplitude-Frequency Characteristics of Ladder Networks, Marconi's Wireless Telegraph Co., Essex, England; 1954.

11. J. K. Skwirzynski and J. Zdunek, "Design Data for Symmetrical Darlington Filters," Proc. IRE, vol. 104, pt. c (Sept. 1957) pp. 366-380.

12. S. D. Bedrosin, E. L. Luke, and H. N. Putchi, "On the Tabulation of Insertion Loss Low-Pass Chain Matrix Coefficient and Network Element Values," Proc. Natl. Electronics Conf., vol. 11, (1955) pp. 697-717.

13. T. Laurent, Vierpoltherie und Frequenztransformation, Springer-Verlag, Berlin, 1956.

14. H. W. Bode, Network Analysis and Feedback Amplifier Design, D. van Nostrand Company, Inc., New York, 1945.

15. T. E. Shea, Transmission Networks and Wave Filters, D. van Nostrand Company, Inc., New York, 1929.

16. F. Scowen, Introduction to Theory and Design of Electric Wave Filters, Chapman & Hall, Ltd., London 1950.

17. W.H. Chen, Elements of Electrical Analysis and Synthesis, McGraw Hill Co. In press.

18. A. C. Bartlett, The Theory of Electrical Artificial Lines and Filters, John Wiley & Sons, New York, 1931.

19. V. Belevitch, "Tchebycheff Filters and Amplifier Networks," Wireless Engineer, vol. 29 (April 1952) p. 106.

20. L. M. Milne - Thomson, Die elliptischen Funktionen von Jacobi, Springer Verlag, Berlin, 1931.

21. E. Jahnke and F. Emde, Tables of Functions, Dover Publications, New York, 1945.

22. W. N. Tuttle, "Design of Two-Section Symmetrical Zobel Filters for Tchebycheff Insertion Loss," Proc. IRE, vol. 47 (Jan. 1959), pp. 29-36.

23. E. Glowatzki, "Sechsstellige Tafel der Cauer-Parameter," Abhandlungen der Bayerischen Akademie fer Wissenschaften, Neue Folge, Heft 67 (1955).

24. W. Saraga, "Insertion Loss and Insertion Phase-Shift of Multi-section Zobel Filters with Equal Image Impedances," P.O. Elec. Eng. J., vol. 39 (Jan. 1947), pp. 167-172.

25. W. N. Tuttle, "Applied Circuit Theory," IRE Trans. on Circuit Theory, vol. CT - 4, (June 1957) pp. 29-32.

26. J. H. Mole, Filter Design Data, John Wiley and Sons, Inc., New York, 1952.

BIOGRAPHY

David Silber was born on October 2, 1922, in Lodz, Poland. His undergraduate studies were pursued at the O.V.M. Polytechnikum in Munich, Germany, from which he received the degree of Electrical Engineer in June, 1950.

After arrival in the United States in 1951, he pursued graduate studies at the University of Cincinnati, Evening College and Summer School, while employed by the Keleket X-Ray Corporation in Covington, Kentucky. Since 1954 he has been employed by the Communication Accessories Company in Kansas City, Missouri, taking leave in 1956 to enter the University of Florida for further graduate studies.

At the University of Florida he held a graduate fellowship for two years and taught electrical engineering for one year. He received the degree of Master of Science in Engineering in August, 1957.

This dissertation was prepared under the direction of the chairman of the candidate's supervisory committee and has been approved by all members of that committee. It was submitted to the Dean of the College of Engineering and to the Graduate Council, and was approved as partial fulfillment of the requirements for the degree of Doctor of Philosophy.

August 13, 1960

Dean, College of Engineering

Dean, Graduate School

SUPERVISORY COMMITTEE:

Chairman

E. E. Muschlitz, Jr.

W. H. Chen

D. E. Seeley

R. G. Blake

3 1262 07332 052 4